EUROPEAN ORGANIZATION FOR NUCLEAR RESEARCH

Skewness and kurtosis of mean transverse momentum fluctuations at the LHC energies

ALICE Collaboration*

Abstract

The first measurements of skewness and kurtosis of mean transverse momentum ($\langle p_T \rangle$) fluctuations are reported in Pb–Pb collisions at $\sqrt{s_{NN}} = 5.02$ TeV, Xe–Xe collisions at $\sqrt{s_{NN}} = 5.44$ TeV and pp collisions at $\sqrt{s} = 5.02$ TeV using the ALICE detector. The measurements are carried out as a function of system size $\langle \mathrm{d}N_{ch}/\mathrm{d}\eta \rangle^{1/3}_{|\eta|<0.5}$, using charged particles with transverse momentum (p_T) and pseudorapidity (η), in the range $0.2 < p_T < 3.0$ GeV/c and $|\eta| < 0.8$, respectively. In Pb–Pb and Xe–Xe collisions, positive skewness is observed in the fluctuations of $\langle p_T \rangle$ for all centralities, which is significantly larger than what would be expected in the scenario of independent particle emission. This positive skewness is considered a crucial consequence of the hydrodynamic evolution of the hot and dense nuclear matter created in heavy-ion collisions. Furthermore, similar observations of positive skewness for minimum bias pp collisions are also reported here. Kurtosis of $\langle p_T \rangle$ fluctuations is found to be in good agreement with the kurtosis of Gaussian distribution, for most central Pb–Pb collisions. Hydrodynamic model calculations with MUSIC using Monte Carlo Glauber initial conditions are able to explain the measurements of both skewness and kurtosis qualitatively from semicentral to central collisions in Pb–Pb system. Color reconnection mechanism in PYTHIA8 model seems to play a pivotal role in capturing the qualitative behavior of the same measurements in pp collisions.

---

*See Appendix A for the list of collaboration members

arXiv:2308.16217v1 [nucl-ex] 30 Aug 2023

1 Introduction

The properties of the hot and dense nuclear matter created in heavy-ion collisions at relativistic energies can be studied using event-by-event fluctuations of different quantities like multiplicity, net-charge, mean transverse momentum ($\langle p_T \rangle$), etc. [1–4]. The analysis of event-by-event fluctuations of these variables offers valuable means to probe the dynamical fluctuations that originate from the production of a quark–gluon plasma (QGP) [5] phase during heavy-ion collisions. Fluctuations in the thermodynamic quantity of temperature, which are associated with the phase transition in the quantum chromodynamics (QCD) phase diagram, can manifest themselves in the fluctuations of the $\langle p_T \rangle$ of the final-state particles [6]. A non-monotonic behavior of $\langle p_T \rangle$ fluctuations as a function of centrality or incident energy was suggested as one of the possible signals of the QGP [3]. However, $\langle p_T \rangle$ fluctuations are also affected by non-thermodynamic variations in the initial geometry of the collision that include fluctuations in the initial size, shape and orientation of the colliding nuclei, and the fluctuating number of nucleons participating in the collision. The $\langle p_T \rangle$ fluctuations measured at RHIC did not show any beam energy dependence, and the non-monotonic behavior with centrality was also not observed [7]. The previous measurements of $\langle p_T \rangle$ fluctuations in Pb–Pb collisions at centre-of-mass energy per nucleon pair, $\sqrt{s_{NN}} = 2.76$ TeV in ALICE [8] suggested a connection of the observed fluctuations of the $\langle p_T \rangle$ to the fluctuations in the initial state of the collision. Qualitatively, the data obtained from model calculations using the string melting approach in A Multi-Phase Transport (AMPT) model [9], where partons rescatter and recombine through a hadronic coalescence scheme, exhibit agreement with the observed results [8]. The string melting version was introduced in the model [10] to address and account for the effects of flow originating from the entire partonic system in the overlap volume of heavy-ion collisions, as opposed to considering only the contributions from minijet partons in the default version. By incorporating the string melting approach, the model was able to simulate the collective behavior of the partonic system during the early stages of the collision, leading to a more accurate description of the experimental observations of elliptic flow. The $\langle p_T \rangle$ fluctuations were also calculated in the color glass condensate (CGC) [11, 12] formulation, where they have been related to initial spatial fluctuations of glasma flux tube via their coupling to a collective flow field. The comparison of these calculations with data showed a good agreement in the semicentral and central collisions [13].

The space–time evolution of the QGP phase produced in the relativistic heavy-ion collisions is well described by the relativistic viscous hydrodynamics [14–16]. In Ref. [17], it has been proposed that the skewness of $\langle p_T \rangle$ fluctuations can serve as an essential probe of the hydrodynamic behavior of the system created in heavy-ion collisions. The $\langle p_T \rangle$ of the particles emitted at freeze-out was found to be correlated to the initial energy of the system at the beginning of the hydrodynamic evolution, instead of the energy of the system at freeze-out [18]. The fluctuations of $\langle p_T \rangle$ are therefore found to be related to the fluctuations of initial energy density in an *effective* hydrodynamic description [19]. It was shown that the skewness of $\langle p_T \rangle$ fluctuations are driven by the skewness of the initial energy density fluctuations, which implies that the $\langle p_T \rangle$ fluctuations arise from the same collective dynamics in the QGP phase that give rise to anisotropic flow. Furthermore, employing initial conditions from the T$_R$ENTo model [20] and evolving them with the V-USPHYDRO viscous hydrodynamic [21] simulations predicted positive skewness of $\langle p_T \rangle$ fluctuations surpassing expectations in independent particle emission scenarios. Additional information regarding these simulations can be found in Ref. [17].

The fluctuations in $\langle p_T \rangle$ of charged particles can be influenced by various physical effects, such as collective behavior of the system formed in the collisions, fluctuations in the number of participating nucleons, the presence of jets, or other non-Gaussian fluctuations. Examining the higher-order terms of $\langle p_T \rangle$ fluctuations will enable us to delve deeper into the intricate mechanisms underlying the observed fluctuations and acquire valuable insights. In this article, the first experimental study of skewness and kurtosis of $\langle p_T \rangle$ fluctuations that represent the third- and fourth-order fluctuations of $\langle p_T \rangle$ are reported at the Large Hadron Collider (LHC) energies. The observables used in this analysis are introduced in Sec. 2. Here,

the multiparticle p_T correlators used to study the $\langle p_\mathrm{T} \rangle$ fluctuations are defined. A brief description of the subsystems of ALICE detector relevant to this analysis is given in Sec. 3. The analysis technique and the method of estimating statistical and systematic uncertainties for the measurements are explained in Sec. 4. The skewness and the kurtosis of $\langle p_\mathrm{T} \rangle$ fluctuations as a function of system size and the interpretation of results using theoretical models are presented in Sec. 5. The major findings of the analysis are summarized in Sec. 6.

2 Observables

In this analysis, the fluctuations in event-by-event $\langle p_\mathrm{T} \rangle$ of charged particles are investigated using multi-particle p_T correlators. The event-by-event $\langle p_\mathrm{T} \rangle$ is defined as

$$\langle p_\mathrm{T} \rangle = \frac{\sum_{i=1}^{N_\mathrm{ch}} p_{\mathrm{T},i}}{N_\mathrm{ch}}, \tag{1}$$

where $p_{\mathrm{T},i}$ is the transverse momentum of the ith particle and N_ch is the total number of charged particles in the event. Alternatively, one can employ the standard moment method for event-by-event analysis of $\langle p_\mathrm{T} \rangle$ fluctuations. The moment method calculates various order moments of the $\langle p_\mathrm{T} \rangle$ distribution, providing a comprehensive evaluation of the total fluctuation accounting for both the statistical and dynamical (non-statistical) parts. The advantage of employing multiparticle p_T correlators [22, 23] is that they yield zero values for events with randomly sampled particles, thereby effectively isolating the non-statistical fluctuations of interest. The expressions for the two-particle p_T correlator ($\langle \Delta p_{\mathrm{T},i} \Delta p_{\mathrm{T},j} \rangle$) and three-particle p_T correlator ($\langle \Delta p_{\mathrm{T},i} \Delta p_{\mathrm{T},j} \Delta p_{\mathrm{T},k} \rangle$) [17] are denoted by Eqs. 2 and 3, respectively, where Q_n is given by Eq. 5. Constraints on the indices in summations in the definition of correlators ensure that self-correlations are eliminated. The algebraic expressions of the correlators in terms of Q_n's where $n = 1, 2, ..$ were derived to account for the practical limitations of calculating multiparticle p_T correlators with nested loops, especially when dealing with events characterized by large multiplicities. Since, the values of Q_n can be obtained with Eq. 5 employing a single loop, it becomes feasible to directly utilize the later expressions with Q_ns in Eqs. 2 and 3 for the calculation of two- and three-particle p_T correlators, respectively. On similar lines, the four-particle p_T correlator ($\langle \Delta p_{\mathrm{T},i} \Delta p_{\mathrm{T},j} \Delta p_{\mathrm{T},k} \Delta p_{\mathrm{T},l} \rangle$) is derived as shown in Eq. 4. These correlators are related to the variance, skewness, and kurtosis of the $\langle p_\mathrm{T} \rangle$ distribution.

$$\langle \Delta p_{\mathrm{T},i} \Delta p_{\mathrm{T},j} \rangle = \left\langle \frac{\sum_{\substack{i,j, \\ i \neq j}}^{N_\mathrm{ch}} (p_{\mathrm{T},i} - \langle\langle p_\mathrm{T} \rangle\rangle)(p_{\mathrm{T},j} - \langle\langle p_\mathrm{T} \rangle\rangle)}{N_\mathrm{ch}(N_\mathrm{ch}-1)} \right\rangle_\mathrm{ev} = \left\langle \frac{Q_1^2 - Q_2}{N_\mathrm{ch}(N_\mathrm{ch}-1)} \right\rangle_\mathrm{ev} - \left\langle \frac{Q_1}{N_\mathrm{ch}} \right\rangle_\mathrm{ev}^2, \tag{2}$$

$$\langle \Delta p_{\mathrm{T},i} \Delta p_{\mathrm{T},j} \Delta p_{\mathrm{T},k} \rangle = \left\langle \frac{\sum_{\substack{i,j,k, \\ i \neq j \neq k}}^{N_\mathrm{ch}} (p_{\mathrm{T},i} - \langle\langle p_\mathrm{T} \rangle\rangle)(p_{\mathrm{T},j} - \langle\langle p_\mathrm{T} \rangle\rangle)(p_{\mathrm{T},k} - \langle\langle p_\mathrm{T} \rangle\rangle)}{N_\mathrm{ch}(N_\mathrm{ch}-1)(N_\mathrm{ch}-2)} \right\rangle_\mathrm{ev}$$
$$= \left\langle \frac{Q_1^3 - 3Q_2 Q_1 + 2Q_3}{N_\mathrm{ch}(N_\mathrm{ch}-1)(N_\mathrm{ch}-2)} \right\rangle_\mathrm{ev} - 3 \left\langle \frac{Q_1^2 - Q_2}{N_\mathrm{ch}(N_\mathrm{ch}-1)} \right\rangle_\mathrm{ev} \left\langle \frac{Q_1}{N_\mathrm{ch}} \right\rangle_\mathrm{ev} + 2 \left\langle \frac{Q_1}{N_\mathrm{ch}} \right\rangle_\mathrm{ev}^3, \tag{3}$$

$$\langle \Delta p_{\mathrm{T},i} \Delta p_{\mathrm{T},j} \Delta p_{\mathrm{T},k} \Delta p_{\mathrm{T},l} \rangle = \left\langle \frac{\sum_{\substack{i,j,k,l, \\ i \neq j \neq k \neq l}}^{N_\mathrm{ch}} (p_{\mathrm{T},i} - \langle\langle p_\mathrm{T} \rangle\rangle)(p_{\mathrm{T},j} - \langle\langle p_\mathrm{T} \rangle\rangle)(p_{\mathrm{T},k} - \langle\langle p_\mathrm{T} \rangle\rangle)(p_{\mathrm{T},l} - \langle\langle p_\mathrm{T} \rangle\rangle)}{N_\mathrm{ch}(N_\mathrm{ch}-1)(N_\mathrm{ch}-2)(N_\mathrm{ch}-3)} \right\rangle_\mathrm{ev}$$

$$= \left\langle \frac{Q_1^4 - 6Q_4 + 8Q_1Q_3 - 6Q_1^2 Q_2 + 3Q_2^2}{N_{\mathrm{ch}}(N_{\mathrm{ch}} - 1)(N_{\mathrm{ch}} - 2)(N_{\mathrm{ch}} - 3)} \right\rangle_{\mathrm{ev}}$$

$$- 4 \left\langle \frac{Q_1^3 - 3Q_2Q_1 + 2Q_3}{N_{\mathrm{ch}}(N_{\mathrm{ch}} - 1)(N_{\mathrm{ch}} - 2)} \right\rangle_{\mathrm{ev}} \left\langle \frac{Q_1}{N_{\mathrm{ch}}} \right\rangle_{\mathrm{ev}}$$

$$+ 6 \left\langle \frac{Q_1^2 - Q_2}{N_{\mathrm{ch}}(N_{\mathrm{ch}} - 1)} \right\rangle_{\mathrm{ev}} \left\langle \frac{Q_1}{N_{\mathrm{ch}}} \right\rangle_{\mathrm{ev}}^2 - 3 \left\langle \frac{Q_1}{N_{\mathrm{ch}}} \right\rangle_{\mathrm{ev}}^4 , \tag{4}$$

$$Q_n = \sum_{i=1}^{N_{\mathrm{ch}}} p_{\mathrm{T},i}^n . \tag{5}$$

In the above equations, angular brackets $\langle \ldots \rangle_{\mathrm{ev}}$ denote an average over all events and $\langle\langle p_T \rangle\rangle = \langle Q_1/N_{\mathrm{ch}} \rangle_{\mathrm{ev}}$ is the event-by-event $\langle p_T \rangle$ averaged over events. The standardized skewness ($\gamma_{\langle p_T \rangle}$) and the intensive skewness ($\Gamma_{\langle p_T \rangle}$) are two measures of the skewness of the $\langle p_T \rangle$ distribution, constructed using the two-particle and three-particle p_T correlators [17], given by

$$\gamma_{\langle p_T \rangle} = \frac{\langle \Delta p_{\mathrm{T},i} \Delta p_{\mathrm{T},j} \Delta p_{\mathrm{T},k} \rangle}{\langle \Delta p_{\mathrm{T},i} \Delta p_{\mathrm{T},j} \rangle^{3/2}} , \tag{6}$$

and

$$\Gamma_{\langle p_T \rangle} = \frac{\langle \Delta p_{\mathrm{T},i} \Delta p_{\mathrm{T},j} \Delta p_{\mathrm{T},k} \rangle \langle\langle p_T \rangle\rangle}{\langle \Delta p_{\mathrm{T},i} \Delta p_{\mathrm{T},j} \rangle^2} . \tag{7}$$

The kurtosis $\kappa_{\langle p_T \rangle}$ of $\langle p_T \rangle$ distribution is defined as

$$\kappa_{\langle p_T \rangle} = \frac{\langle \Delta p_{\mathrm{T},i} \Delta p_{\mathrm{T},j} \Delta p_{\mathrm{T},k} \Delta p_{\mathrm{T},l} \rangle}{\langle \Delta p_{\mathrm{T},i} \Delta p_{\mathrm{T},j} \rangle^2} . \tag{8}$$

The article focuses on analyzing higher order fluctuations of $\langle p_T \rangle$, particularly the third and fourth order. Three key observables, namely the standardized skewness, intensive skewness, and kurtosis of the $\langle p_T \rangle$ distribution (defined in Eqs. 6, 7, and 8, respectively), are investigated as a function of the system size in Pb–Pb collisions at $\sqrt{s_{\mathrm{NN}}} = 5.02$ TeV, Xe–Xe collisions at $\sqrt{s_{\mathrm{NN}}} = 5.44$ TeV, and pp collisions at $\sqrt{s} = 5.02$ TeV.

3 Experimental setup

The measurements reported in the article are obtained using the data recorded by the ALICE detector at the LHC. A detailed description of the ALICE detector and its performance can be found in Refs. [24, 25]. The primary sub-detectors relevant to this analysis are the Time Projection Chamber (TPC) [26], the Inner Tracking System (ITS) [25], and the V0 detector [27]. The TPC and ITS are used for tracking and reconstructing the primary vertex, while the V0 detector is used for triggering and the default centrality estimation. The V0 detector consists of two scintillator arrays, V0A and V0C, located on both sides of the interaction point, covering the pseudorapidity (η) intervals $2.8 < \eta < 5.1$ and $-3.7 < \eta < -1.7$, respectively [27]. The data analyzed here are obtained from Pb–Pb collisions at $\sqrt{s_{\mathrm{NN}}} = 5.02$ TeV, Xe–Xe collisions at $\sqrt{s_{\mathrm{NN}}} = 5.44$ TeV, and pp collisions at $\sqrt{s} = 5.02$ TeV. These datasets were recorded in 2015 (pp and Pb–Pb) and 2017 (Xe–Xe) during LHC Run 2. A minimum bias (MB) trigger condition is applied to select collision events that requires at least one hit in both the V0A and the V0C detectors. Events that pass the MB trigger criteria and have a reconstructed primary vertex position within 10 cm along the beam axis to the nominal interaction point are selected in the analysis. Using information from multiple detectors as described in Ref. [25], events with more than one reconstructed primary interaction
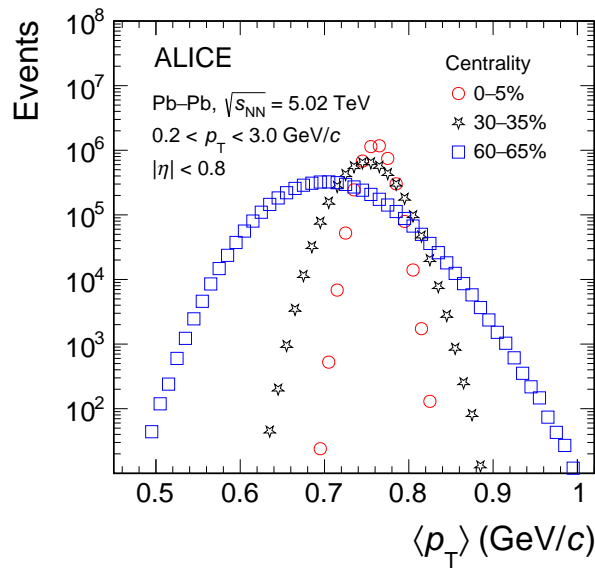
Figure 1: Efficiency uncorrected mean transverse momentum distributions for different centrality classes in Pb–Pb collisions at $\sqrt{s_{NN}} = 5.02$ TeV.

vertex (pile-up events) are rejected. In total, 84 million Pb–Pb collisions, 1.2 million Xe–Xe collisions, and 95 million pp collisions pass the above mentioned criteria and are used for the analysis.

The charged-particle tracks reconstructed using the ITS and the TPC in the ALICE central barrel are selected in the kinematic range $0.2 < p_T < 3.0$ GeV/c and $|\eta| < 0.8$, where p_T is the track momentum in the plane transverse to the beam axis. The accepted tracks exhibit approximately uniform azimuthal acceptance in this region. The tracks that have at least 70 out of a maximum possible 159 reconstructed space points in the TPC, and at least one hit in the two innermost layers of the ITS (ITS has in total six layers) are selected. This selection assures a resolution better than 300 μm [25] on the distance-of-closest-approach (DCA) to the primary vertex in the plane perpendicular (DCA$_{xy}$) and parallel (DCA$_z$) to the beam axis for the selected tracks. In order to suppress the contamination from secondary particles, the DCA of the tracks to the primary vertex must be within 1 cm in the longitudinal direction and 0.1 cm in the transverse plane. Moreover, the χ^2 per degree of freedom of the track fit to the space points in the TPC and the ITS are required to be less than 4 (2.5 for Pb–Pb) and 36, respectively.

4 Data analysis

The mean transverse momentum $\langle p_T \rangle$ distributions obtained for three different centrality classes in Pb–Pb collisions at $\sqrt{s_{NN}} = 5.02$ TeV are shown in Fig. 1. The distributions are not corrected for detector inefficiencies. The centrality classes are formed by splitting the events based on the measured amplitude distribution in the V0A and V0C detectors as described in Refs. [28, 29]. The mean of the $\langle p_T \rangle$ distributions are found to increase whereas the width of the distribution decreases from peripheral to central collisions. The larger width of the distribution for peripheral (lower multiplicity) collisions indicates larger fluctuations compared to the central (higher multiplicity) collisions. Similar behavior is observed in Xe–Xe collisions at $\sqrt{s_{NN}} = 5.44$ TeV and pp collisions at $\sqrt{s} = 5.02$ TeV.

Before starting the analysis with the $\langle p_T \rangle$ correlators presented in Sec. 2, it is important to demonstrate that these fluctuations are not a trivial consequence of fluctuating N_{ch} in a given centrality class. The definition of $\langle p_T \rangle$ in Eq. 1 clearly shows that the varying multiplicity in different events of the same centrality class can affect the $\langle p_T \rangle$ distributions and consequently its fluctuations. To examine whether
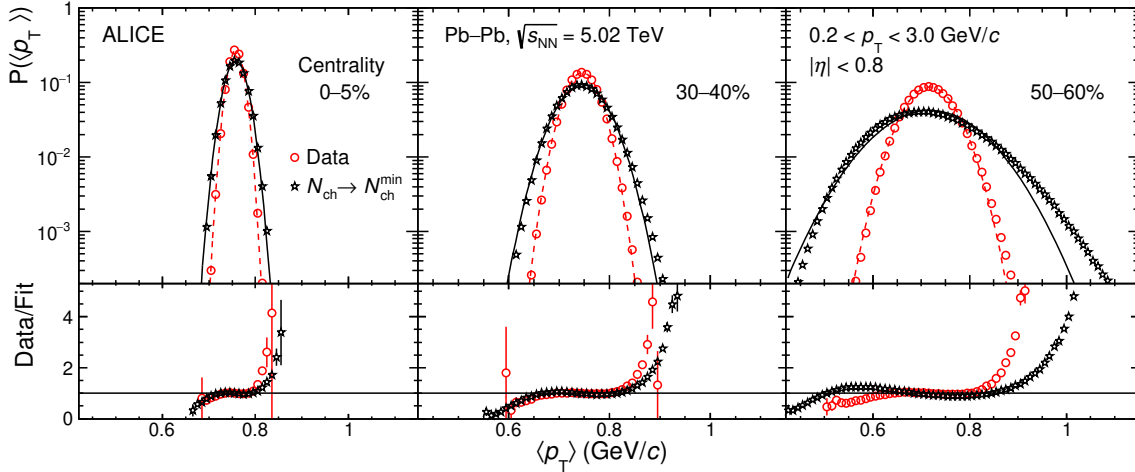
Figure 2: Comparison of event-by-event mean transverse momentum $\langle p_T \rangle$ distribution from actual analysis and modified analysis in which $N_{\rm ch}$ in each event is fixed to $N_{\rm ch}^{\rm min}$ ($N_{\rm ch}^{\rm min}$ is the minimum number of charged particles in a given centrality class) and $N_{\rm ch}^{\rm min}$ number of particles are selected in each event randomly for the 0–5% (left), 30–40% (middle), and 50–60% (right) centrality classes. The lines indicate Gaussian functions.

these fluctuations persist after removing the stochastic effects of the multiplicity, a check is performed. For each centrality class, the minimum number of tracks per event in the kinematic acceptance of the analysis, $N_{\rm ch}^{\rm min}$ is determined. In each event of the centrality class, the $N_{\rm ch}^{\rm min}$ number of tracks are then selected randomly to calculate the genuine $\langle p_T \rangle$ distribution free from biases of multiplicity fluctuations. The left panel of Fig. 2 shows the $\langle p_T \rangle$ distribution for the 0–5% central events in Pb–Pb collisions at $\sqrt{s_{\rm NN}} = 5.02$ TeV. The distribution in red markers shows the original event-by-event $\langle p_T \rangle$ distribution in which $N_{\rm ch}$ fluctuates whereas the distribution shown with black markers is the $\langle p_T \rangle$ distribution in which $N_{\rm ch}$ is fixed to $N_{\rm ch}^{\rm min}$ in each event of the centrality class. A Gaussian function is used to fit the two distributions and the ratio of data to fit is shown in the bottom panel of Fig. 2. The ratio shows that the data points are above the fit in the right-side of the distribution, and below the fit in the left-side, indicating that the $\langle p_T \rangle$ distributions are positively skewed. The $\langle p_T \rangle$ distributions exhibit substantial deviations from a Gaussian distribution even under the condition of a fixed $N_{\rm ch}$, thereby reflecting the analogous traits observed in the original distribution with fluctuating $N_{\rm ch}$. The middle and right panels of Fig. 2 visually exemplify the consistent manifestation of these characteristics within the distributions of $\langle p_T \rangle$ for both semicentral and peripheral collisions. It is concluded that the positive skewness in the event-by-event $\langle p_T \rangle$ distributions is not a trivial consequence of event-by-event statistical fluctuations of $N_{\rm ch}$, and therefore new and non-trivial information can be extracted from higher-order moments of $\langle p_T \rangle$ fluctuations.

The $\langle p_T \rangle$ correlators described in Eqs. 2, 3, and 4 are calculated using charged-particle tracks in different centrality (multiplicity) classes. For Pb–Pb collisions, the observables are analyzed in 18 equal-width centrality classes ranging between zero to ninety percent, i.e., 0–5%, 5–10%, ..., 85–90%. For Xe–Xe collisions, the total number of events are divided into four centrality classes, 0–20%, 20–40%, 40–60%, and 60–80%. The centrality classes are taken wider for Xe–Xe collisions because of the limited data sample. In pp collisions, the events are classified into ten multiplicity classes, 0–1%, 1–5%, 5–10%, 10–15%, 15–20%, 20–30%, 30–40%, 40–50%, 50–70%, and 70–100%. The method of defining these multiplicity classes can be found in Ref. [30].

The $\langle p_T \rangle$ correlators are calculated in the unit multiplicity bins of a given centrality class, and then merged using centrality bin width correction formula [31]. In this way, both the effects of multiplicity fluctuations, and the necessity of using non-trivial multiplicity weight to determine all-event averages

Table 1: Contributions to the total systematic uncertainty on standardized skewness $\gamma_{\langle p_T \rangle}$, intensive skewness $\Gamma_{\langle p_T \rangle}$, and kurtosis $\kappa_{\langle p_T \rangle}$ in Pb–Pb collisions at $\sqrt{s_{NN}} = 5.02$ TeV, Xe–Xe collisions at $\sqrt{s_{NN}} = 5.44$ TeV, and pp collisions at $\sqrt{s} = 5.02$ TeV. Ranges are given where the uncertainties depend on centrality or multiplicity.

Observables	Sources of systematic uncertainty	Pb–Pb	Xe–Xe	pp
$\gamma_{\langle p_T \rangle}$	Event selection	0.9–6.4%	1.6–9.2%	0.3–0.8%
	Track selection	1.6–5.4%	7.4–15.8%	1.0–2.2%
	MC closure	2.3%	2.6%	2.7%
	Total	2.9–8.7%	9.1–17.2%	2.9–3.6%
$\Gamma_{\langle p_T \rangle}$	Event selection	1.6–5.2%	1.7–9.1%	0.3–0.8%
	Track selection	1.0–6.4%	7.6–16.2%	0.7–1.9%
	MC closure	3.6%	2.3%	0.4%
	Total	4–9%	9.5–17.6%	0.8–2.1%
$\kappa_{\langle p_T \rangle}$	Event selection	0.2–5.8%	0.9–4.5%	0.1–1.4%
	Track selection	0.3–4.4%	2.2–10.7%	1.8–4.4%
	MC closure	0.3%	1.3%	0.9%
	Total	0.5–7.3%	2.7–11.7% %	1.8–4.7%

from single-event averages, are eliminated. The statistical uncertainties are evaluated using the bootstrap method. By repeatedly resampling the dataset and analyzing each resample, the bootstrap method provides a robust and computationally feasible approach for estimating the uncertainties associated with the observed results. It allows for a comprehensive assessment of the variability in the data, taking into account the inherent fluctuations and dependencies present in the measurements. The systematic uncertainties on the observables are estimated separately for each collision system by varying event and track selection criteria. The uncertainties related to the event selection include the variation of the accepted vertex position along the beam direction. The uncertainties due to track selection include the variation of the selection criteria on DCA_{xy}, DCA_z, the number of reconstructed space points in the TPC, and the quality of the track fit from their nominal values. Systematic uncertainties obtained from the contribution of each of these sources are considered as uncorrelated and the total systematic uncertainty on the observables is obtained by adding them in quadrature. Table 1 shows the summary of the contributions to the total systematic uncertainty on standardized skewness, intensive skewness, and kurtosis in Pb–Pb, Xe–Xe, and pp collisions.

The standardized skewness, intensive skewness, and kurtosis reported in this draft are considered robust and independent of detection efficiencies [17]. The detector inefficiencies cancel to leading order within these ratios, despite their potential presence in individual p_T correlators. Consequently, efficiency correction is not carried out for these ratios. The robustness of the measured ratios is further affirmed by performing a Monte Carlo (MC) closure test. The MC closure test uses simulations based on different event generators for producing particles that corresponds to generated (true) results and GEANT3 [32] for the transport of particles through the geometry of ALICE detectors. For Pb–Pb and Xe–Xe collisions, the MC events are generated using HIJING (Heavy-Ion Jet Interaction Generator) [33] whereas for pp collisions, the events are produced by PYTHIA8 [34, 35] event generator with Monash2013 tune. The experimental conditions prevailing during the data taking are accounted for in the generated events using GEANT3 by reproducing the actual configuration of different detectors during the runs. Results obtained from the generated events are compared with their corresponding reconstructed ones (without applying efficiency corrections), and they show a good agreement within uncertainties. The ratio of the reconstructed to the generated results for the observables are fitted with zeroth-order polynomial functions to quantify the amount of closure obtained. The percentages of agreement for standardized skewness, intensive skewness, and kurtosis are 97.3%, 99.6% and 99.1%, respectively, in pp collisions at $\sqrt{s} = 5.02$ TeV.

Similar study is also performed for the other two collision systems, Pb–Pb collisions at $\sqrt{s_{\mathrm{NN}}} = 5.02$ and Xe–Xe collisions at $\sqrt{s_{\mathrm{NN}}} = 5.44$ TeV. The percentages of closure for the observables (standardized skewness, intensive skewness, kurtosis) in Pb–Pb (Xe–Xe) collisions are found to be 97.7% (97.4%), 96.4% (97.7%), and 99.7% (98.7%). These differences are added to the systematic uncertainties and reported in Table 1.

To study how the skewness and kurtosis of $\langle p_{\mathrm{T}} \rangle$ distributions vary with the size of the collision system and to have a comparison between heavy-ion collisions (Pb–Pb and Xe–Xe) and small systems like pp collisions, expressing the centrality (multiplicity for pp collisions) classes as average charged particle multiplicity density ($\langle \mathrm{d}N_{\mathrm{ch}}/\mathrm{d}\eta \rangle_{|\eta|<0.5}$) is more suitable. The conversion of centrality to $\langle \mathrm{d}N_{\mathrm{ch}}/\mathrm{d}\eta \rangle_{|\eta|<0.5}$ is performed using the measured values of $\langle \mathrm{d}N_{\mathrm{ch}}/\mathrm{d}\eta \rangle_{|\eta|<0.5}$ for certain centrality classes from Ref. [36] for Pb–Pb collisions. It should be noted that the centrality classes used in this analysis are narrower and different from that in the reference. A linear relation is observed between average number of charged particles ($\langle N_{\mathrm{acc}} \rangle$) in the kinematic range ($|\eta| < 0.8$ and $0.2 < p_{\mathrm{T}} < 0.3$ GeV/c) of this analysis and $\langle \mathrm{d}N_{\mathrm{ch}}/\mathrm{d}\eta \rangle_{|\eta|<0.5}$ over the full centrality range. The extracted fit parameters from the linear relation between $\langle N_{\mathrm{acc}} \rangle$ and $\langle \mathrm{d}N_{\mathrm{ch}}/\mathrm{d}\eta \rangle_{|\eta|<0.5}$ were used to assign a value of $\langle \mathrm{d}N_{\mathrm{ch}}/\mathrm{d}\eta \rangle_{|\eta|<0.5}$ for any value of $\langle N_{\mathrm{acc}} \rangle$. Hence, by calculating the $\langle N_{\mathrm{acc}} \rangle$ for the centrality classes of this analysis, the corresponding value of $\langle \mathrm{d}N_{\mathrm{ch}}/\mathrm{d}\eta \rangle_{|\eta|<0.5}$ is obtained. This method was previously used in the study of second-order fluctuations of $\langle p_{\mathrm{T}} \rangle$ in Ref. [8]. Similar approach is followed for Xe–Xe collisions using $\langle \mathrm{d}N_{\mathrm{ch}}/\mathrm{d}\eta \rangle_{|\eta|<0.5}$ values of centrality classes from Ref. [37]. For pp collisions, the measured values of $\langle \mathrm{d}N_{\mathrm{ch}}/\mathrm{d}\eta \rangle_{|\eta|<0.5}$ are taken from Ref. [30] since the multiplicity classes are the same.

5 Results

5.1 Standardized skewness

The standardized skewness of charged particles produced in Pb–Pb collisions at $\sqrt{s_{\mathrm{NN}}} = 5.02$ TeV and Xe–Xe collisions at $\sqrt{s_{\mathrm{NN}}} = 5.44$ TeV as a function of system size denoted by the cubic root of average charged particle multiplicity density, $\langle \mathrm{d}N_{\mathrm{ch}}/\mathrm{d}\eta \rangle_{|\eta|<0.5}^{1/3}$ is shown in Fig. 3. The femtoscopic radii associated with the radius of the fireball at freeze-out, scale linearly with $\langle \mathrm{d}N_{\mathrm{ch}}/\mathrm{d}\eta \rangle_{|\eta|<0.5}^{1/3}$ and therefore it is used as a proxy for the system size [38]. The uncertainties on $\langle \mathrm{d}N_{\mathrm{ch}}/\mathrm{d}\eta \rangle_{|\eta|<0.5}^{1/3}$ are obtained by propagating the uncertainty on $\langle \mathrm{d}N_{\mathrm{ch}}/\mathrm{d}\eta \rangle_{|\eta|<0.5}$. It is observed that $\gamma_{\langle p_{\mathrm{T}} \rangle}$ decreases with increasing $\langle \mathrm{d}N_{\mathrm{ch}}/\mathrm{d}\eta \rangle_{|\eta|<0.5}^{1/3}$ for both Pb–Pb and Xe–Xe collisions. This can be attributed to statistical fluctuations. If the fluctuations are purely statistical and generated by finite multiplicity (N), then $\gamma_{\langle p_{\mathrm{T}} \rangle}$ would have a dependence of $1/\sqrt{N}$. A slight enhancement of $\gamma_{\langle p_{\mathrm{T}} \rangle}$ in the most central ($\langle \mathrm{d}N_{\mathrm{ch}}/\mathrm{d}\eta \rangle_{|\eta|<0.5}^{1/3} > 11$) Pb–Pb collisions is also observed within uncertainty. One of the probable reasons could be the reduction of two-particle correlations $\langle \Delta p_i \Delta p_j \rangle$ towards the central collisions reported previously in Ref. [8]. Hydrodynamic model calculations from Ref. [17] that uses $\mathrm{T_R ENT_o}$ initial conditions evolved by hydrodynamic code V-USPHYDRO referred as V-USPHYDRO model in the figures are compared with the data for both Pb–Pb and Xe–Xe collisions. A small specific shear viscosity, $\eta/s = 0.047$ is used in the V-USPHYDRO model. As shown in Fig. 3, the V-USPHYDRO model calculations capture the general system size dependence of the measurement, but fail to describe it quantitatively. In the model, $\gamma_{\langle p_{\mathrm{T}} \rangle}$ is larger in Pb–Pb collisions compared to Xe–Xe collisions for almost all multiplicities, however data do not show such system dependence. Model calculations using HIJING [33], which incorporates various phenomena like multiple minijet production with initial and final state radiation or nuclear effects such as parton shadowing and jet quenching, are shown in the figure. HIJING considers nucleus–nucleus collisions as superposition of independent binary collisions of wounded nucleons. The latest version of the model, HIJING/$B\overline{B}$ v2.0 with shadowing and jet quenching effects [39] is used. The $\gamma_{\langle p_{\mathrm{T}} \rangle}$ in HIJING model exhibits a strong dependence with $\langle \mathrm{d}N_{\mathrm{ch}}/\mathrm{d}\eta \rangle_{|\eta|<0.5}^{1/3}$ and reproduces the measurement in the semiperiph-
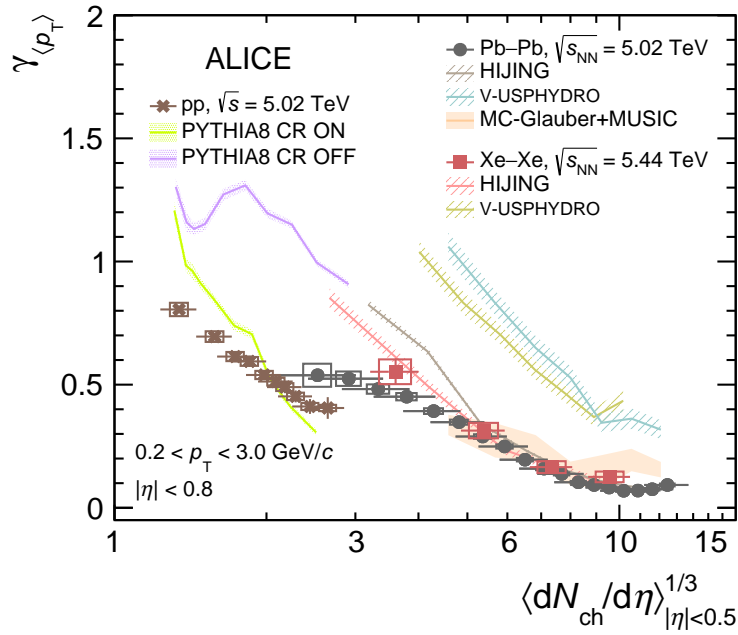
Figure 3: Left: Standardized skewness $\gamma_{\langle p_T \rangle}$ shown as a function of $\langle \mathrm{d}N_{\mathrm{ch}}/\mathrm{d}\eta \rangle^{1/3}_{|\eta|<0.5}$ in Pb–Pb collisions at $\sqrt{s_{\mathrm{NN}}} = 5.02$ TeV, Xe–Xe collisions at $\sqrt{s_{\mathrm{NN}}} = 5.44$ TeV, and pp collisions at $\sqrt{s} = 5.02$ TeV. The predictions from different event generators and hydrodynamic model calculations from V-USPHYDRO [17] and MC-Glauber+MUSIC [40, 41] are denoted by colored bands. The statistical (systematic) uncertainties are represented by vertical bars (boxes).

eral to semicentral region. Calculations performed using the MC-Glauber+MUSIC model, which adopts the Glauber Monte Carlo [40] approach to generate initial conditions for the collisions, followed by the MUSIC hydrodynamic model [41] with $\eta/s = 0.1$ are presented. Notably, both the HIJING and MC-Glauber+MUSIC model utilize the Monte Carlo Glauber initial conditions, with the primary difference lying in the subsequent evolution. While HIJING lacks the implementation of collective phenomena, MUSIC incorporates such effects. Interestingly, the results obtained for the $\gamma_{\langle p_T \rangle}$ in Pb–Pb collisions remain same for both models from peripheral to semicentral collisions. This prompts the question of whether the $\gamma_{\langle p_T \rangle}$ is primarily sensitive to the details of the initial conditions.

The results in Pb–Pb and Xe–Xe are also compared with the measurements carried out in pp collisions at $\sqrt{s} = 5.02$ TeV. The $\gamma_{\langle p_T \rangle}$ in pp collisions shows a steeper decrease with increasing $\langle \mathrm{d}N_{\mathrm{ch}}/\mathrm{d}\eta \rangle^{1/3}_{|\eta|<0.5}$ compared to heavy-ion collisions. The observed $\gamma_{\langle p_T \rangle}$ is also found smaller in pp collisions than in Pb–Pb collisions for a given $\langle \mathrm{d}N_{\mathrm{ch}}/\mathrm{d}\eta \rangle^{1/3}_{|\eta|<0.5}$. The measurements in pp collisions are compared with PYTHIA8 [35] model, which is a pQCD based MC event generator. The PYTHIA8 model is found to describe numerous experimental results in pp collisions at LHC energies quite successfully [42–44]. This model can involve color reconnection (CR) mechanism [45] in pp collisions, which could contribute to explaining certain collective effects that have been observed in these collisions. Comparison of the measurements in pp collisions with PYTHIA8 model for both cases, with and without enabling CR mechanism (referred as PYTHIA8 CR ON and PYTHIA8 CR OFF), are presented. PYTHIA8 CR OFF model calculations utterly fail to describe the measurements both qualitatively and quantitatively. On the other hand, PYTHIA CR ON calculations reproduce the dependence of $\gamma_{\langle p_T \rangle}$ with $\langle \mathrm{d}N_{\mathrm{ch}}/\mathrm{d}\eta \rangle^{1/3}_{|\eta|<0.5}$ although with a larger slope.

9
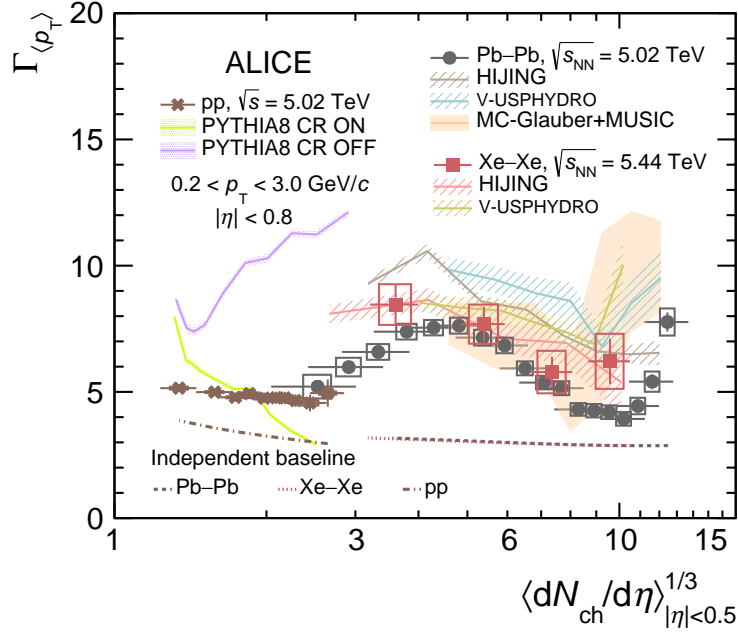
Figure 4: Intensive skewness $\Gamma_{\langle p_{\mathrm{T}} \rangle}$ shown as a function of $\langle \mathrm{d}N_{\mathrm{ch}}/\mathrm{d}\eta \rangle^{1/3}_{|\eta|<0.5}$ in Pb–Pb collisions at $\sqrt{s_{\mathrm{NN}}} = 5.02$ TeV, Xe–Xe collisions at $\sqrt{s_{\mathrm{NN}}} = 5.44$ TeV, and pp collisions at $\sqrt{s} = 5.02$ TeV. The colored dashed lines represent the independent baseline for each system. The predictions from different event generators and hydrodynamic model calculations from V-USPHYDRO [17] and MC-Glauber+MUSIC [40, 41] are denoted by colored bands. The statistical (systematic) uncertainties are represented by vertical bars (boxes).

5.2 Intensive skewness

The left panel of Fig. 4 shows the intensive skewness studied with respect to $\langle \mathrm{d}N_{\mathrm{ch}}/\mathrm{d}\eta \rangle^{1/3}_{|\eta|<0.5}$ in Pb–Pb collisions at $\sqrt{s_{\mathrm{NN}}} = 5.02$ TeV and Xe–Xe collisions at $\sqrt{s_{\mathrm{NN}}} = 5.44$ TeV. The colored dashed lines indicate the independent baselines $\Gamma_{\mathrm{independent}}$ evaluated for each system separately. The formula [17] used to calculate the independent baseline for intensive skewness is

$$\Gamma_{\mathrm{independent}} = \frac{\langle (p_{\mathrm{T}} - \langle p_{\mathrm{T}} \rangle)^3 \rangle \langle p_{\mathrm{T}} \rangle}{\langle (p_{\mathrm{T}} - \langle p_{\mathrm{T}} \rangle)^2 \rangle^2} \quad , \tag{9}$$

where $\langle p_{\mathrm{T}} \rangle$ is the average transverse momentum in given centrality class. The p_{T} spectra for different centrality classes are the input distributions for the calculation of $\Gamma_{\mathrm{independent}}$ as a function of centrality. The second and third central moments of the p_{T} distributions, $\langle (p_{\mathrm{T}} - \langle p_{\mathrm{T}} \rangle)^2 \rangle$ and $\langle (p_{\mathrm{T}} - \langle p_{\mathrm{T}} \rangle)^3 \rangle$ are evaluated using the p_{T} spectrum for each centrality class and the ratio of these moments gives the $\Gamma_{\mathrm{independent}}$ for that centrality class. For Pb–Pb and Xe–Xe collisions, the p_{T} spectra are taken from Refs. [46] and [47], respectively. Consecutively, the centralities are converted into $\langle \mathrm{d}N_{\mathrm{ch}}/\mathrm{d}\eta \rangle_{|\eta|<0.5}$ and $\langle \mathrm{d}N_{\mathrm{ch}}/\mathrm{d}\eta \rangle^{1/3}_{|\eta|<0.5}$. A positive intensive skewness, larger than the independent baseline, is observed in both Pb–Pb and Xe–Xe collisions as a function of system size. This observation is in accordance with the predictions from the V-USPHYDRO hydrodynamic model calculations. The V-USPHYDRO model results describe the data qualitatively but do not show quantitative agreement. The HIJING model calculations though seem to capture the decreasing trend of the measurements in the semiperipheral to semicentral region ($3.8 \leq \langle \mathrm{d}N_{\mathrm{ch}}/\mathrm{d}\eta \rangle^{1/3}_{|\eta|<0.5} \leq 8.9$) but are unable to explain the rise of $\Gamma_{\langle p_{\mathrm{T}} \rangle}$ in the measurements from the semicentral to central region ($9.0 \leq \langle \mathrm{d}N_{\mathrm{ch}}/\mathrm{d}\eta \rangle^{1/3}_{|\eta|<0.5} \leq 12.4$). The observed increase in both $\gamma_{\langle p_{\mathrm{T}} \rangle}$ and $\Gamma_{\langle p_{\mathrm{T}} \rangle}$ for $\langle \mathrm{d}N_{\mathrm{ch}}/\mathrm{d}\eta \rangle^{1/3}_{|\eta|<0.5} > 11$ in Pb–Pb collsions might be indicative of the onset of thermalization [48, 49]. The MC-Glauber+MUSIC model calculations exhibit similar behavior observed in

the measurements of $\Gamma_{\langle p_T \rangle}$ in Pb–Pb collisions and provide better agreement quantitatively than the V-USPHYDRO model results. The increase of $\Gamma_{\langle p_T \rangle}$ for central collisions in the measurements, seems to be depicted by both of the hydrodynamic model calculations with different initial conditions and therfore demands theoretical inputs to understand this rise.

The measurement performed in pp collisions at $\sqrt{s} = 5.02$ TeV is also shown along with its independent baseline. For pp collisions, the baseline is calculated using the p_T spectra from Ref. [50]. The hydrodynamic prediction of positive intensive skewness above of its baseline is pronounced in the measurements in pp collisions as well. The distinct non-monotonic behavior observed in Pb–Pb collisions as a function of $\langle dN_{ch}/d\eta \rangle^{1/3}_{|\eta|<0.5}$ is noticeably attenuated in pp collisions. The $\Gamma_{\langle p_T \rangle}$ exhibits a subtle, monotonic decrease as $\langle dN_{ch}/d\eta \rangle^{1/3}_{|\eta|<0.5}$ increases in pp collisions. In the PYTHIA8 CR OFF model, the results for $\Gamma_{\langle p_T \rangle}$ exhibit an increase as $\langle dN_{ch}/d\eta \rangle^{1/3}_{|\eta|<0.5}$ increases, which is in direct contrast to the observations from the PYTHIA8 CR ON model. While the PYTHIA8 CR ON model appears to be in closer agreement with the experimental measurements compared to CR OFF, neither model adequately captures the qualitative behavior observed in the measurements.

5.3   Kurtosis

The kurtosis evaluated using Eq. 4 as a function of $\langle dN_{ch}/d\eta \rangle^{1/3}_{|\eta|<0.5}$ in Pb–Pb collisions at $\sqrt{s_{NN}} = 5.02$ TeV and Xe–Xe collisions at $\sqrt{s_{NN}} = 5.44$ TeV is shown in Fig. 5. The $\kappa_{\langle p_T \rangle}$ for a Gaussian distribution, which serves as a baseline for independent particle production, is shown with dotted line. The $\kappa_{\langle p_T \rangle}$ is found to decrease with increasing system size in Pb–Pb and Xe–Xe collisions and approaches the Gaussian baseline towards the most central Pb–Pb collisions. The measurements are compared with HIJING model calculations for both Pb–Pb and Xe–Xe collisions. While the HIJING model successfully capture the decreasing trend observed in the measurements with respect to $\langle dN_{ch}/d\eta \rangle^{1/3}_{|\eta|<0.5}$, it exhibits a pronounced and rapid decrease in $\kappa_{\langle p_T \rangle}$ compared to the data points. This is related to trivial system size dependence of $\kappa_{\langle p_T \rangle}$ in HIJING that should follow $1/N$ dependence. Throughout the entire range of $\langle dN_{ch}/d\eta \rangle^{1/3}_{|\eta|<0.5}$, the HIJING model overestimates the measurements. The MC-Glauber+MUSIC calculations reproduce the measurements in the central to midperipheral region ($5.4 \leq \langle dN_{ch}/d\eta \rangle^{1/3}_{|\eta|<0.5} \leq 12.4$). The measurements in pp collisions at $\sqrt{s} = 5.02$ TeV are also shown in the Fig. 5. In pp collisions, the $\kappa_{\langle p_T \rangle}$ decreases with $\langle dN_{ch}/d\eta \rangle^{1/3}_{|\eta|<0.5}$ and remains consistently above the Gaussian baseline even for the highest value of $\langle dN_{ch}/d\eta \rangle^{1/3}_{|\eta|<0.5}$. Calculations of $\kappa_{\langle p_T \rangle}$ in PYTHIA8 show similar behavior with $\langle dN_{ch}/d\eta \rangle^{1/3}_{|\eta|<0.5}$ as in data when CR mechanism is turned ON. PYTHIA8 CR OFF model completely fails to describe the measured $\kappa_{\langle p_T \rangle}$.

6   Summary

In summary, first results on higher order fluctuations of mean transverse momentum ($\langle p_T \rangle$) of charged particles, skewness, and kurtosis in Pb–Pb, Xe–Xe, and pp collisions at LHC energies are presented. Two measures of skewness, standardized skewness and intensive skewness, are studied using three- and two-particle p_T correlators as a function of system size ($\langle dN_{ch}/d\eta \rangle^{1/3}_{|\eta|<0.5}$). The standardized skewness is found to decrease with increasing system size in all three collision systems. Positive intensive skewness, larger than the baseline and constant with the predictions from the hydrodynamics studies in Ref. [17], is observed in both Pb–Pb and Xe–Xe collisions. The same feature as observed in A–A collisions is reported in pp collisions. HIJING model calculations, which do not incorporate hydrodynamic evolution, are able to exhibit the qualitative behavior of intensive skewness in the region of $3.8 \leq \langle dN_{ch}/d\eta \rangle^{1/3}_{|\eta|<0.5} \leq 8.9$. The striking rise of intensive skewness in the most central region is unexplained by HIJING. This effect is, however captured in the hydrodynamic calculations of both V-
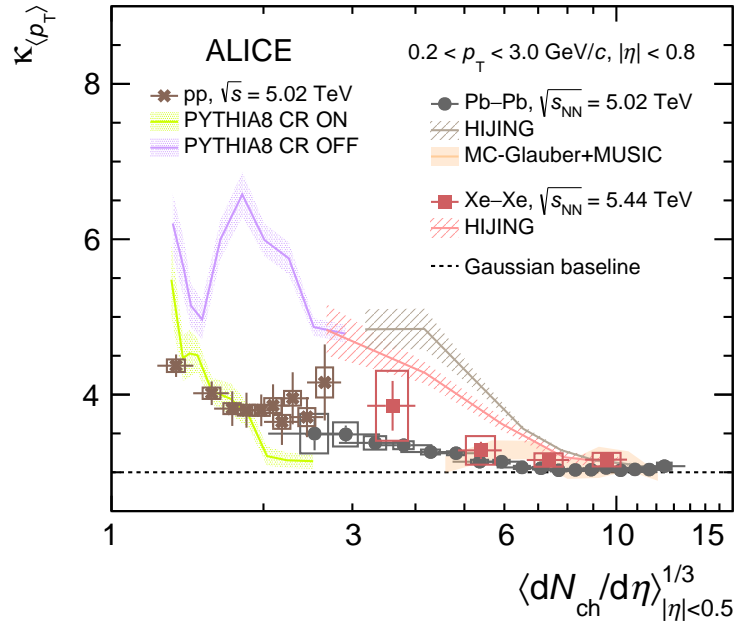
Figure 5: Left: Kurtosis $\kappa_{\langle p_T \rangle}$ shown as a function of $\langle \mathrm{d}N_{\mathrm{ch}}/\mathrm{d}\eta \rangle_{|\eta|<0.5}^{1/3}$ in Pb–Pb collisions at $\sqrt{s_{\mathrm{NN}}} = 5.02$ TeV, Xe–Xe collisions at $\sqrt{s_{\mathrm{NN}}} = 5.44$ TeV and pp collisions at $\sqrt{s} = 5.02$ TeV. The predictions from different event generators and hydrodynamic calculations from MC-Glauber+MUSIC model [40, 41] are represented by colored bands. The dashed line indicates the Gaussian baseline. The statistical (systematic) uncertainties are represented by vertical bars (boxes).

USPHYDRO and MC-Glauber+MUSIC models. The MC-Glauber+MUSIC model shows good agreement with the measurements of the standardized skewness and intensive skewness in the region of 4.8 $\leq \langle \mathrm{d}N_{\mathrm{ch}}/\mathrm{d}\eta \rangle_{|\eta|<0.5}^{1/3} \leq 12.4$. In contrast, the V-USPHYDRO model, which utilizes T$_R$ENTo initial conditions, overestimates both measures of skewness. The discrepancy between the results obtained from the two hydrodynamic models suggests that these measurements can provide valuable insights into the initial stages of the collision. Also, the standardized skewness in HIJING and MC-Glauber+MUSIC models exhibits similar behavior, suggesting that its sensitivity may primarily be attributed to the details of the initial conditions rather than the subsequent evolution. In pp collisions, the PYTHIA8 model with the color reconnection mechanism enabled is able to qualitatively reproduce the measurements. The kurtosis measured using the two- and four-particle p_T correlators shows a decrease with the system size. This decreasing behavior is reproduced by the HIJING model calculations in Pb–Pb and Xe–Xe collisions, which, however, do not show a quantitative agreement with the measurements. Hydrodynamic calculations from MC-Glauber+MUSIC model explain the measurement well in the region of 4.8 $\leq \langle \mathrm{d}N_{\mathrm{ch}}/\mathrm{d}\eta \rangle_{|\eta|<0.5}^{1/3} \leq 12.4$. The value of kurtosis from the MC-Glauber+MUSIC model has a similar value to that from a Gaussian distribution. The measurements of kurtosis in Pb–Pb collisions also agreeing with the Gaussian baseline for highest values of the system size, hint about the production of a locally thermalized system in most central Pb–Pb collisions.

Acknowledgements

12

References

[1] E. V. Shuryak, "Event per event analysis of heavy ion collisions and thermodynamical fluctuations", *Phys. Lett. B* **423** (1998) 9–14, `arXiv:hep-ph/9704456`.

[2] M. A. Stephanov, K. Rajagopal, and E. V. Shuryak, "Event-by-event fluctuations in heavy ion collisions and the QCD critical point", *Phys. Rev. D* **60** (1999) 114028, `arXiv:hep-ph/9903292`.

[3] H. Heiselberg, "Event-by-event physics in relativistic heavy ion collisions", *Phys. Rept.* **351** (2001) 161–194, `arXiv:nucl-th/0003046`.

[4] **ALICE** Collaboration, "The ALICE experiment – A journey through QCD", *CERN-EP-2022-227* (11, 2022) , `arXiv:2211.04384 [nucl-ex]`.

[5] E. V. Shuryak, "Quark-Gluon Plasma and Hadronic Production of Leptons, Photons and Psions", *Phys. Lett. B* **78** (1978) 150.

[6] L. Stodolsky, "Temperature fluctuations in multiparticle production", *Phys. Rev. Lett.* **75** (1995) 1044–1045.

[7] **STAR** Collaboration, J. Adams *et al.*, "Incident energy dependence of pt correlations at RHIC", *Phys. Rev. C* **72** (2005) 044902, `arXiv:nucl-ex/0504031`.

[8] **ALICE** Collaboration, B. Abelev *et al.*, "Event-by-event mean $p_\mathbf{T}$ fluctuations in pp and Pb-Pb collisions at the LHC", *Eur. Phys. J. C* **74** (2014) 3077, `arXiv:1407.5530 [nucl-ex]`.

[9] Z.-W. Lin, C. M. Ko, B.-A. Li, B. Zhang, and S. Pal, "A Multi-phase transport model for relativistic heavy ion collisions", *Phys. Rev. C* **72** (2005) 064901, `arXiv:nucl-th/0411110`.

[10] C. Zhang, L. Zheng, F. Liu, S. Shi, and Z.-W. Lin, "Update of a multiphase transport model with modern parton distribution functions and nuclear shadowing", *Phys. Rev. C* **99** (2019) 064906, `arXiv:1903.03292 [nucl-th]`.

[11] F. Gelis, E. Iancu, J. Jalilian-Marian, and R. Venugopalan, "The Color Glass Condensate", *Ann. Rev. Nucl. Part. Sci.* **60** (2010) 463–489, `arXiv:1002.0333 [hep-ph]`.

[12] H. Weigert, "Evolution at small x(bj): The Color glass condensate", *Prog. Part. Nucl. Phys.* **55** (2005) 461–565, `arXiv:hep-ph/0501087`.

[13] S. Gavin and G. Moschelli, "Fluctuation Probes of Early-Time Correlations in Nuclear Collisions", *Phys. Rev. C* **85** (2012) 014905, `arXiv:1107.3317 [nucl-th]`.

[14] S. Bhadury, M. Kurian, V. Chandra, and A. Jaiswal, "Second order relativistic viscous hydrodynamics within an effective description of hot QCD medium", *J. Phys. G* **48** (2021) 105104, `arXiv:2010.01537 [hep-ph]`.

[15] U. Heinz, C. Shen, and H. Song, "The viscosity of quark-gluon plasma at RHIC and the LHC", *AIP Conf. Proc.* **1441** (2012) 766–770, `arXiv:1108.5323 [nucl-th]`.

[16] P. Romatschke, "New Developments in Relativistic Viscous Hydrodynamics", *Int. J. Mod. Phys. E* **19** (2010) 1–53, `arXiv:0902.3663 [hep-ph]`.

[17] G. Giacalone, F. G. Gardim, J. Noronha-Hostler, and J.-Y. Ollitrault, "Skewness of mean transverse momentum fluctuations in heavy-ion collisions", *Phys. Rev. C* **103** (2021) 024910, `arXiv:2004.09799 [nucl-th]`.

[18] F. G. Gardim, G. Giacalone, M. Luzum, and J.-Y. Ollitrault, "Effects of initial state fluctuations on the mean transverse momentum", *Nucl. Phys. A* **1005** (2021) 121999, `arXiv:2002.07008` `[nucl-th]`.

[19] F. G. Gardim, G. Giacalone, M. Luzum, and J.-Y. Ollitrault, "Thermodynamics of hot strong-interaction matter from ultrarelativistic nuclear collisions", *Nature Phys.* **16** (2020) 615–619, `arXiv:1908.09728` `[nucl-th]`.

[20] J. S. Moreland, J. E. Bernhard, and S. A. Bass, "Alternative ansatz to wounded nucleon and binary collision scaling in high-energy nuclear collisions", *Phys. Rev. C* **92** (2015) 011901, `arXiv:1412.4708` `[nucl-th]`.

[21] J. Noronha-Hostler, G. S. Denicol, J. Noronha, R. P. G. Andrade, and F. Grassi, "Bulk Viscosity Effects in Event-by-Event Relativistic Hydrodynamics", *Phys. Rev. C* **88** (2013) 044916, `arXiv:1305.1981` `[nucl-th]`.

[22] **STAR** Collaboration, S. A. Voloshin, "Multiplicity and mean transverse momentum fluctuations in Au+Au collisions at RHIC", *AIP Conf. Proc.* **610** (2002) 591–596, `arXiv:nucl-ex/0109006`.

[23] S. A. Voloshin, "Mean p(t) fluctuations from two particle and four particle correlations", `arXiv:nucl-th/0206052`.

[24] **ALICE** Collaboration, K. Aamodt *et al.*, "The ALICE experiment at the CERN LHC", *JINST* **3** (2008) S08002.

[25] **ALICE** Collaboration, B. Abelev *et al.*, "Performance of the ALICE Experiment at the CERN LHC", *Int. J. Mod. Phys. A* **29** (2014) 1430044, `arXiv:1402.4476` `[nucl-ex]`.

[26] J. Alme *et al.*, "The ALICE TPC, a large 3-dimensional tracking device with fast readout for ultra-high multiplicity events", *Nucl. Instrum. Meth. A* **622** (2010) 316–367, `arXiv:1001.1950` `[physics.ins-det]`.

[27] **ALICE** Collaboration, E. Abbas *et al.*, "Performance of the ALICE VZERO system", *JINST* **8** (2013) P10016, `arXiv:1306.3130` `[nucl-ex]`.

[28] **ALICE** Collaboration, ALICE, "Centrality determination in heavy ion collisions", *ALICE-PUBLIC-2018-011* (2018) . `http://cds.cern.ch/record/2636623`.

[29] **ALICE** Collaboration, ALICE, "Centrality determination using the Glauber model in Xe-Xe collisions at $\sqrt{s_{\mathrm{NN}}} = 5.44$ TeV", *ALICE-PUBLIC-2018-003* (2018) . `https://cds.cern.ch/record/2315401`.

[30] **ALICE** Collaboration, S. Acharya *et al.*, "Pseudorapidity distributions of charged particles as a function of mid- and forward rapidity multiplicities in pp collisions at $\sqrt{s} = 5.02$, 7 and 13 TeV", *Eur. Phys. J. C* **81** (2021) 630, `arXiv:2009.09434` `[nucl-ex]`.

[31] X. Luo, J. Xu, B. Mohanty, and N. Xu, "Volume fluctuation and auto-correlation effects in the moment analysis of net-proton multiplicity distributions in heavy-ion collisions", *J. Phys. G* **40** (2013) 105104, `arXiv:1302.2332` `[nucl-ex]`.

[32] R. Brun, F. Bruyant, F. Carminati, S. Giani, M. Maire, A. McPherson, G. Patrick, and L. Urban, "GEANT Detector Description and Simulation Tool", *CERN-W5013* (10, 1994) . `http://cds.cern.ch/record/1082634`.

[33] X.-N. Wang and M. Gyulassy, "HIJING: A Monte Carlo model for multiple jet production in p p, p A and A A collisions", *Phys. Rev. D* **44** (1991) 3501–3516.

[34] T. Sjöstrand, S. Mrenna, and P. Z. Skands, "PYTHIA 6.4 Physics and Manual", *JHEP* **05** (2006) 026, `arXiv:hep-ph/0603175`.

[35] T. Sjöstrand, S. Ask, J. R. Christiansen, R. Corke, N. Desai, P. Ilten, S. Mrenna, S. Prestel, C. O. Rasmussen, and P. Z. Skands, "An introduction to PYTHIA 8.2", *Comput. Phys. Commun.* **191** (2015) 159–177, `arXiv:1410.3012 [hep-ph]`.

[36] **ALICE** Collaboration, J. Adam *et al.*, "Centrality dependence of the charged-particle multiplicity density at midrapidity in Pb-Pb collisions at $\sqrt{s_{NN}}$ = 5.02 TeV", *Phys. Rev. Lett.* **116** (2016) 222302, `arXiv:1512.06104 [nucl-ex]`.

[37] **ALICE** Collaboration, S. Acharya *et al.*, "Centrality and pseudorapidity dependence of the charged-particle multiplicity density in Xe–Xe collisions at $\sqrt{s_{NN}}$ =5.44TeV", *Phys. Lett. B* **790** (2019) 35–48, `arXiv:1805.04432 [nucl-ex]`.

[38] **ALICE** Collaboration, K. Aamodt *et al.*, "Two-pion Bose-Einstein correlations in central Pb-Pb collisions at $\sqrt{s_{NN}}$ = 2.76 TeV", *Phys. Lett. B* **696** (2011) 328–337, `arXiv:1012.4035 [nucl-ex]`.

[39] V. Topor Pop, M. Gyulassy, J. Barrette, C. Gale, X. N. Wang, and N. Xu, "Baryon junction loops and the baryon-meson anomaly at high energies", *Phys. Rev. C* **70** (2004) 064906, `arXiv:nucl-th/0407095`.

[40] B. Alver, M. Baker, C. Loizides, and P. Steinberg, "The PHOBOS Glauber Monte Carlo", `arXiv:0805.4411 [nucl-ex]`.

[41] B. Schenke, S. Jeon, and C. Gale, "(3+1)D hydrodynamic simulation of relativistic heavy-ion collisions", *Phys. Rev. C* **82** (2010) 014903, `arXiv:1004.1408 [hep-ph]`.

[42] **ALICE** Collaboration, J. Adam *et al.*, "Charged-particle multiplicities in proton–proton collisions at $\sqrt{s}$ = 0.9 to 8 TeV", *Eur. Phys. J. C* **77** (2017) 33, `arXiv:1509.07541 [nucl-ex]`.

[43] **ALICE** Collaboration, S. Acharya *et al.*, "Charged-particle multiplicity distributions over a wide pseudorapidity range in proton-proton collisions at $\sqrt{s}$ = 0.9, 7, and 8 TeV", *Eur. Phys. J. C* **77** (2017) 852, `arXiv:1708.01435 [hep-ex]`.

[44] **ALICE** Collaboration, B. Abelev *et al.*, "Multiplicity dependence of the average transverse momentum in pp, p-Pb, and Pb-Pb collisions at the LHC", *Phys. Lett. B* **727** (2013) 371–380, `arXiv:1307.1094 [nucl-ex]`.

[45] T. Sjostrand and M. van Zijl, "A Multiple Interaction Model for the Event Structure in Hadron Collisions", *Phys. Rev. D* **36** (1987) 2019.

[46] **ALICE** Collaboration, S. Acharya *et al.*, "Transverse momentum spectra and nuclear modification factors of charged particles in pp, p-Pb and Pb-Pb collisions at the LHC", *JHEP* **11** (2018) 013, `arXiv:1802.09145 [nucl-ex]`.

[47] **ALICE** Collaboration, S. Acharya *et al.*, "Transverse momentum spectra and nuclear modification factors of charged particles in Xe-Xe collisions at $\sqrt{s_{NN}}$ = 5.44 TeV", *Phys. Lett. B* **788** (2019) 166–179, `arXiv:1805.04399 [nucl-ex]`.

[48] R. Samanta, S. Bhatta, J. Jia, M. Luzum, and J.-Y. Ollitrault, "Thermalization at the femtoscale seen in high-energy Pb+Pb collisions", `arXiv:2303.15323 [nucl-th]`.

[49] R. Samanta, J. a. P. Picchetti, M. Luzum, and J.-Y. Ollitrault, "Non-Gaussian transverse momentum fluctuations from impact parameter fluctuations", `arXiv:2306.09294 [nucl-th]`.

[50] **ALICE** Collaboration, S. Acharya *et al.*, "Charged-particle production as a function of multiplicity and transverse spherocity in pp collisions at $\sqrt{s} = 5.02$ and 13 TeV", *Eur. Phys. J. C* **79** (2019) 857, arXiv:1905.07208 [nucl-ex].

A   The ALICE Collaboration

S. Acharya [126], D. Adamová [86], G. Aglieri Rinella [33], M. Agnello [30], N. Agrawal [51], Z. Ahammed [134], S. Ahmad [16], S.U. Ahn [71], I. Ahuja [38], A. Akindinov [142], M. Al-Turany [97], D. Aleksandrov [142], B. Alessandro [56], H.M. Alfanda [6], R. Alfaro Molina [67], B. Ali [16], A. Alici [26], N. Alizadehvandchali [115], A. Alkin [33], J. Alme [21], G. Alocco [52], T. Alt [64], A.R. Altamura [50], I. Altsybeev [95], M.N. Anaam [6], C. Andrei [46], N. Andreou [114], A. Andronic [137], V. Anguelov [94], F. Antinori [54], P. Antonioli [51], N. Apadula [74], L. Aphecetche [103], H. Appelshäuser [64], C. Arata [73], S. Arcelli [26], M. Aresti [23], R. Arnaldi [56], J.G.M.C.A. Arneiro [110], I.C. Arsene [20], M. Arslandok [139], A. Augustinus [33], R. Averbeck [97], M.D. Azmi [16], H. Baba [123], A. Badalà [53], J. Bae [104], Y.W. Baek [41], X. Bai [119], R. Bailhache [64], Y. Bailung [48], A. Balbino [30], A. Baldisseri [129], B. Balis [2], D. Banerjee [4], Z. Banoo [91], R. Barbera [27], F. Barile [32], L. Barioglio [95], M. Barlou[78], B. Barman[42], G.G. Barnaföldi [138], L.S. Barnby [85], V. Barret [126], L. Barreto [110], C. Bartels [118], K. Barth [33], E. Bartsch [64], N. Bastid [126], S. Basu [75], G. Batigne [103], D. Battistini [95], B. Batyunya [143], D. Bauri[47], J.L. Bazo Alba [101], I.G. Bearden [83], C. Beattie [139], P. Becht [97], D. Behera [48], I. Belikov [128], A.D.C. Bell Hechavarria [137], F. Bellini [26], R. Bellwied [115], S. Belokurova [142], Y.A.V. Beltran [45], G. Bencedi [138], S. Beole [25], Y. Berdnikov [142], A. Berdnikova [94], L. Bergmann [94], M.G. Besoiu [63], L. Betev [33], P.P. Bhaduri [134], A. Bhasin [91], M.A. Bhat [4], B. Bhattacharjee [42], L. Bianchi [25], N. Bianchi [49], J. Bielčík [36], J. Bielčíková [86], J. Biernat [107], A.P. Bigot [128], A. Bilandzic [95], G. Biro [138], S. Biswas [4], N. Bize [103], J.T. Blair [108], D. Blau [142], M.B. Blidaru [97], N. Bluhme[39], C. Blume [64], G. Boca [22,55], F. Bock [87], T. Bodova [21], A. Bogdanov[142], S. Boi [23], J. Bok [58], L. Boldizsár [138], M. Bombara [38], P.M. Bond [33], G. Bonomi [133,55], H. Borel [129], A. Borissov [142], A.G. Borquez Carcamo [94], H. Bossi [139], E. Botta [25], Y.E.M. Bouziani [64], L. Bratrud [64], P. Braun-Munzinger [97], M. Bregant [110], M. Broz [36], G.E. Bruno [96,32], M.D. Buckland [24], D. Budnikov [142], H. Buesching [64], S. Bufalino [30], P. Buhler [102], N. Burmasov [142], Z. Buthelezi [68,122], A. Bylinkin [21], S.A. Bysiak[107], M. Cai [6], H. Caines [139], A. Caliva [29], E. Calvo Villar [101], J.M.M. Camacho [109], P. Camerini [24], F.D.M. Canedo [110], M. Carabas [125], A.A. Carballo [33], F. Carnesecchi [33], R. Caron [127], L.A.D. Carvalho [110], J. Castillo Castellanos [129], F. Catalano [33,25], C. Ceballos Sanchez [143], I. Chakaberia [74], P. Chakraborty [47], S. Chandra [134], S. Chapeland [33], M. Chartier [118], S. Chattopadhyay [134], S. Chattopadhyay [99], T.G. Chavez [45], T. Cheng [97,6], C. Cheshkov [127], B. Cheynis [127], V. Chibante Barroso [33], D.D. Chinellato [111], E.S. Chizzali [I,95], J. Cho [58], S. Cho [58], P. Chochula [33], D. Choudhury[42], P. Christakoglou [84], C.H. Christensen [83], P. Christiansen [75], T. Chujo [124], M. Ciacco [30], C. Cicalo [52], F. Cindolo [51], M.R. Ciupek[97], G. Clai[II,51], F. Colamaria [50], J.S. Colburn[100], D. Colella [96,32], M. Colocci [26], M. Concas [III,33], G. Conesa Balbastre [73], Z. Conesa del Valle [130], G. Contin [24], J.G. Contreras [36], M.L. Coquet [129], P. Cortese [132,56], M.R. Cosentino [112], F. Costa [33], S. Costanza [22,55], C. Cot [130], J. Crkovská [94], P. Crochet [126], R. Cruz-Torres [74], P. Cui [6], A. Dainese [54], M.C. Danisch [94], A. Danu [63], P. Das [80], P. Das [4], S. Das [4], A.R. Dash [137], S. Dash [47], R.M.H. David[45], A. De Caro [29], G. de Cataldo [50], J. de Cuveland[39], A. De Falco [23], D. De Gruttola [29], N. De Marco [56], C. De Martin [24], S. De Pasquale [29], R. Deb [133], R. Del Grande [95], L. Dello Stritto [29], W. Deng [6], P. Dhankher [19], D. Di Bari [32], A. Di Mauro [33], B. Diab [129], R.A. Diaz [143,7], T. Dietel [113], Y. Ding [6], J. Ditzel [64], R. Divià [33], D.U. Dixit [19], Ø. Djuvsland[21], U. Dmitrieva [142], A. Dobrin [63], B. Dönigus [64], J.M. Dubinski [135], A. Dubla [97], S. Dudi [90], P. Dupieux [126], M. Durkac[106], N. Dzalaiova[13], T.M. Eder [137], R.J. Ehlers [74], F. Eisenhut [64], R. Ejima[92], D. Elia [50], B. Erazmus [103], F. Ercolessi [26], B. Espagnon [130], G. Eulisse [33], D. Evans [100], S. Evdokimov [142], L. Fabbietti [95], M. Faggin [28], J. Faivre [73], F. Fan [6], W. Fan [74], A. Fantoni [49], M. Fasel [87], A. Feliciello [56], G. Feofilov [142], A. Fernández Téllez [45], L. Ferrandi [110], M.B. Ferrer [33], A. Ferrero [129], C. Ferrero [56], A. Ferretti [25], V.J.G. Feuillard [94], V. Filova [36], D. Finogeev [142], F.M. Fionda [52], E. Flatland[33], F. Flor [115], A.N. Flores [108], S. Foertsch [68], I. Fokin [94], S. Fokin [142], E. Fragiacomo [57], E. Frajna [138], U. Fuchs [33], N. Funicello [29], C. Furget [73], A. Furs [142], T. Fusayasu [98], J.J. Gaardhøje [83], M. Gagliardi [25], A.M. Gago [101], T. Gahlaut[47], C.D. Galvan [109], D.R. Gangadharan [115], P. Ganoti [78], C. Garabatos [97], A.T. Garcia [130], J.R.A. Garcia [45], E. Garcia-Solis [9], C. Gargiulo [33], P. Gasik [97], A. Gautam [117], M.B. Gay Ducati [66], M. Germain [103], A. Ghimouz[124], C. Ghosh[134], M. Giacalone [51], G. Gioachin [30], P. Giubellino [97,56], P. Giubilato [28], A.M.C. Glaenzer [129], P. Glässel [94], E. Glimos [121], D.J.Q. Goh[76], V. Gonzalez [136], P. Gordeev[142], M. Gorgon [2], K. Goswami [48], S. Gotovac[34], V. Grabski [67], L.K. Graczykowski [135], E. Grecka [86], A. Grelli [59], C. Grigoras [33], V. Grigoriev [142], S. Grigoryan [143,1], F. Grosa [33], J.F. Grosse-Oetringhaus [33], R. Grosso [97], D. Grund [36], N.A. Grunwald[94], G.G. Guardiano [111], R. Guernane [73], M. Guilbaud [103], K. Gulbrandsen [83], T. Gündem [64], T. Gunji [123],

W. Guo [6], A. Gupta [91], R. Gupta [91], R. Gupta [48], S.P. Guzman [45], K. Gwizdziel [135], L. Gyulai [138], C. Hadjidakis [130], F.U. Haider [91], S. Haidlova [36], H. Hamagaki [76], A. Hamdi [74], Y. Han [140], B.G. Hanley [136], R. Hannigan [108], J. Hansen [75], M.R. Haque [135], J.W. Harris [139], A. Harton [9], H. Hassan [116], D. Hatzifotiadou [51], P. Hauer [43], L.B. Havener [139], S.T. Heckel [95], E. Hellbär [97], H. Helstrup [35], M. Hemmer [64], T. Herman [36], G. Herrera Corral [8], F. Herrmann [137], S. Herrmann [127], K.F. Hetland [35], B. Heybeck [64], H. Hillemanns [33], B. Hippolyte [128], F.W. Hoffmann [70], B. Hofman [59], G.H. Hong [140], M. Horst [95], A. Horzyk[2], Y. Hou [6], P. Hristov [33], C. Hughes [121], P. Huhn[64], L.M. Huhta [116], T.J. Humanic [88], A. Hutson [115], D. Hutter [39], R. Ilkaev[142], H. Ilyas [14], M. Inaba [124], G.M. Innocenti [33], M. Ippolitov [142], A. Isakov [84,86], T. Isidori [117], M.S. Islam [99], M. Ivanov [97], M. Ivanov[13], V. Ivanov [142], K.E. Iversen [75], M. Jablonski [2], B. Jacak [74], N. Jacazio [26], P.M. Jacobs [74], S. Jadlovska[106], J. Jadlovsky[106], S. Jaelani [82], C. Jahnke [110], M.J. Jakubowska [135], M.A. Janik [135], T. Janson[70], S. Ji [17], S. Jia [10], A.A.P. Jimenez [65], F. Jonas [87], D.M. Jones [118], J.M. Jowett [33,97], J. Jung [64], M. Jung [64], A. Junique [33], A. Jusko [100], M.J. Kabus [33,135], J. Kaewjai[105], P. Kalinak [60], A.S. Kalteyer [97], A. Kalweit [33], V. Kaplin [142], A. Karasu Uysal [72], D. Karatovic [89], O. Karavichev [142], T. Karavicheva [142], P. Karczmarczyk [135], E. Karpechev [142], U. Kebschull [70], R. Keidel [141], D.L.D. Keijdener[59], M. Keil [33], B. Ketzer [43], S.S. Khade [48], A.M. Khan [119], S. Khan [16], A. Khanzadeev [142], Y. Kharlov [142], A. Khatun [117], A. Khuntia [36], B. Kileng [35], B. Kim [104], C. Kim [17], D.J. Kim [116], E.J. Kim [69], J. Kim [140], J.S. Kim [41], J. Kim [58], J. Kim[69], M. Kim [19], S. Kim [18], T. Kim [140], K. Kimura [92], S. Kirsch [64], I. Kisel [39], S. Kiselev [142], A. Kisiel [135], J.P. Kitowski [2], J.L. Klay [5], J. Klein [33], S. Klein [74], C. Klein-Bösing [137], M. Kleiner [64], T. Klemenz [95], A. Kluge [33], A.G. Knospe [115], C. Kobdaj [105], T. Kollegger[97], A. Kondratyev [143], N. Kondratyeva [142], E. Kondratyuk [142], J. Konig [64], S.A. Konigstorfer [95], P.J. Konopka [33], G. Kornakov [135], S.D. Koryciak [2], A. Kotliarov [86], V. Kovalenko [142], M. Kowalski [107], V. Kozhuharov [37], I. Králik [60], A. Kravčáková [38], L. Krcal [33,39], M. Krivda [100,60], F. Krizek [86], K. Krizkova Gajdosova [33], M. Kroesen [94], M. Krüger [64], D.M. Krupova [36], E. Kryshen [142], V. Kučera [58], C. Kuhn [128], P.G. Kuijer [84], T. Kumaoka[124], D. Kumar[134], L. Kumar [90], N. Kumar[90], S. Kumar [32], S. Kundu [33], P. Kurashvili [79], A. Kurepin [142], A.B. Kurepin [142], A. Kuryakin [142], S. Kushpil [86], V. Kuskov[142], M.J. Kweon [58], Y. Kwon [140], S.L. La Pointe [39], P. La Rocca [27], A. Lakrathok[105], M. Lamanna [33], R. Langoy [120], P. Larionov [33], E. Laudi [33], L. Lautner [33,95], R. Lavicka [102], R. Lea [133,55], H. Lee [104], I. Legrand [46], G. Legras [137], J. Lehrbach [39], T.M. Lelek[2], R.C. Lemmon [85], I. León Monzón [109], M.M. Lesch [95], E.D. Lesser [19], P. Lévai [138], X. Li[10], J. Lien [120], R. Lietava [100], I. Likmeta [115], B. Lim [25], S.H. Lim [17], V. Lindenstruth [39], A. Lindner[46], C. Lippmann [97], D.H. Liu [6], J. Liu [118], G.S.S. Liveraro [111], I.M. Lofnes [21], C. Loizides [87], S. Lokos [107], J. Lomker [59], P. Loncar [34], X. Lopez [126], E. López Torres [7], P. Lu [97,119], F.V. Lugo [67], J.R. Luhder [137], M. Lunardon [28], G. Luparello [57], Y.G. Ma [40], M. Mager [33], A. Maire [128], M.V. Makariev [37], M. Malaev [142], G. Malfattore [26], N.M. Malik [91], Q.W. Malik[20], S.K. Malik [91], L. Malinina [VI,143], D. Mallick [130,80], N. Mallick [48], G. Mandaglio [31,53], S.K. Mandal [79], V. Manko [142], F. Manso [126], V. Manzari [50], Y. Mao [6], R.W. Marcjan [2], G.V. Margagliotti [24], A. Margotti [51], A. Marín [97], C. Markert [108], P. Martinengo [33], M.I. Martínez [45], G. Martínez García [103], M.P.P. Martins [110], S. Masciocchi [97], M. Masera [25], A. Masoni [52], L. Massacrier [130], O. Massen [59], A. Mastroserio [131,50], O. Matonoha [75], S. Mattiazzo [28], A. Matyja [107], C. Mayer [107], A.L. Mazuecos [33], F. Mazzaschi [25], M. Mazzilli [33], J.E. Mdhluli [122], Y. Melikyan [44], A. Menchaca-Rocha [67], J.E.M. Mendez [65], E. Meninno [102,29], A.S. Menon [115], M. Meres [13], S. Mhlanga[113,68], Y. Miake[124], L. Micheletti [33], D.L. Mihaylov [95], K. Mikhaylov [143,142], A.N. Mishra [138], D. Miśkowiec [97], A. Modak [4], B. Mohanty[80], M. Mohisin Khan [IV,16], M.A. Molander [44], S. Monira [135], C. Mordasini [116], D.A. Moreira De Godoy [137], I. Morozov [142], A. Morsch [33], T. Mrnjavac [33], V. Muccifora [49], S. Muhuri [134], J.D. Mulligan [74], A. Mulliri[23], M.G. Munhoz [110], R.H. Munzer [64], H. Murakami [123], S. Murray [113], L. Musa [33], J. Musinsky [60], J.W. Myrcha [135], B. Naik [122], A.I. Nambrath [19], B.K. Nandi [47], R. Nania [51], E. Nappi [50], A.F. Nassirpour [18], A. Nath [94], C. Nattrass [121], T.K. Nayak [80,115], M.N. Naydenov [37], A. Neagu[20], A. Negru[125], E. Nekrasova[142], L. Nellen [65], R. Nepeivoda [75], S. Nese [20], G. Neskovic [39], N. Nicassio [50], B.S. Nielsen [83], E.G. Nielsen [83], S. Nikolaev [142], S. Nikulin [142], V. Nikulin [142], F. Noferini [51], S. Noh [12], P. Nomokonov [143], J. Norman [118], N. Novitzky [87], P. Nowakowski [135], A. Nyanin [142], J. Nystrand [21], M. Ogino [76], S. Oh [18], A. Ohlson [75], V.A. Okorokov [142], J. Oleniacz [135], A.C. Oliveira Da Silva [121], A. Onnerstad [116], C. Oppedisano [56], A. Ortiz Velasquez [65], J. Otwinowski [107], M. Oya[92], K. Oyama [76], Y. Pachmayer [94], S. Padhan [47], D. Pagano [133,55], G. Paić [65], A. Palasciano [50], S. Panebianco [129],

19

H. Park [124], H. Park [104], J. Park [58], J.E. Parkkila [33], Y. Patley [47], R.N. Patra[91], B. Paul [23], H. Pei [6], T. Peitzmann [59], X. Peng [11], M. Pennisi [25], S. Perciballi [25], D. Peresunko [142], G.M. Perez [7], Y. Pestov[142], V. Petrov [142], M. Petrovici [46], R.P. Pezzi [103,66], S. Piano [57], M. Pikna [13], P. Pillot [103], O. Pinazza [51,33], L. Pinsky[115], C. Pinto [95], S. Pisano [49], M. Płoskoń [74], M. Planinic[89], F. Pliquett[64], M.G. Poghosyan [87], B. Polichtchouk [142], S. Politano [30], N. Poljak [89], A. Pop [46], S. Porteboeuf-Houssais [126], V. Pozdniakov [143], I.Y. Pozos [45], K.K. Pradhan [48], S.K. Prasad [4], S. Prasad [48], R. Preghenella [51], F. Prino [56], C.A. Pruneau [136], I. Pshenichnov [142], M. Puccio [33], S. Pucillo [25], Z. Pugelova[106], S. Qiu [84], L. Quaglia [25], S. Ragoni [15], A. Rai [139], A. Rakotozafindrabe [129], L. Ramello [132,56], F. Rami [128], S.A.R. Ramirez [45], T.A. Rancien[73], M. Rasa [27], S.S. Räsänen [44], R. Rath [51], M.P. Rauch [21], I. Ravasenga [84], K.F. Read [87,121], C. Reckziegel [112], A.R. Redelbach [39], K. Redlich [V,79], C.A. Reetz [97], A. Rehman[21], F. Reidt [33], H.A. Reme-Ness [35], Z. Rescakova[38], K. Reygers [94], A. Riabov [142], V. Riabov [142], R. Ricci [29], M. Richter [20], A.A. Riedel [95], W. Riegler [33], A.G. Riffero [25], C. Ristea [63], M.V. Rodriguez [33], M. Rodríguez Cahuantzi [45], K. Røed [20], R. Rogalev [142], E. Rogochaya [143], T.S. Rogoschinski [64], D. Rohr [33], D. Röhrich [21], P.F. Rojas[45], S. Rojas Torres [36], P.S. Rokita [135], G. Romanenko [26], F. Ronchetti [49], A. Rosano [31,53], E.D. Rosas[65], K. Roslon [135], A. Rossi [54], A. Roy [48], S. Roy [47], N. Rubini [26], D. Ruggiano [135], R. Rui [24], P.G. Russek [2], R. Russo [84], A. Rustamov [81], E. Ryabinkin [142], Y. Ryabov [142], A. Rybicki [107], H. Rytkonen [116], J. Ryu [17], W. Rzesa [135], O.A.M. Saarimaki [44], S. Sadhu [32], S. Sadovsky [142], J. Saetre [21], K. Šafařík [36], P. Saha[42], S.K. Saha [4], S. Saha [80], B. Sahoo [47], B. Sahoo [48], R. Sahoo [48], S. Sahoo[61], D. Sahu [48], P.K. Sahu [61], J. Saini [134], K. Sajdakova[38], S. Sakai [124], M.P. Salvan [97], S. Sambyal [91], D. Samitz [102], I. Sanna [33,95], T.B. Saramela[110], P. Sarma [42], V. Sarritzu [23], V.M. Sarti [95], M.H.P. Sas [33], S. Sawan[80], J. Schambach [87], H.S. Scheid [64], C. Schiaua [46], R. Schicker [94], F. Schlepper [94], A. Schmah[97], C. Schmidt [97], H.R. Schmidt[93], M.O. Schmidt [33], M. Schmidt[93], N.V. Schmidt [87], A.R. Schmier [121], R. Schotter [128], A. Schröter [39], J. Schukraft [33], K. Schweda [97], G. Scioli [26], E. Scomparin [56], J.E. Seger [15], Y. Sekiguchi[123], D. Sekihata [123], M. Selina [84], I. Selyuzhenkov [97], S. Senyukov [128], J.J. Seo [94,58], D. Serebryakov [142], L. Šerkšnytė [95], A. Sevcenco [63], T.J. Shaba [68], A. Shabetai [103], R. Shahoyan[33], A. Shangaraev [142], A. Sharma[90], B. Sharma [91], D. Sharma [47], H. Sharma [54], M. Sharma [91], S. Sharma [76], S. Sharma [91], U. Sharma [91], A. Shatat [130], O. Sheibani[115], K. Shigaki [92], M. Shimomura[77], J. Shin[12], S. Shirinkin [142], Q. Shou [40], Y. Sibiriak [142], S. Siddhanta [52], T. Siemiarczuk [79], T.F. Silva [110], D. Silvermyr [75], T. Simantathammakul[105], R. Simeonov [37], B. Singh[91], B. Singh [95], K. Singh [48], R. Singh [80], R. Singh [91], R. Singh [48], S. Singh [16], V.K. Singh [134], V. Singhal [134], T. Sinha [99], B. Sitar [13], M. Sitta [132,56], T.B. Skaali[20], G. Skorodumovs [94], M. Slupecki [44], N. Smirnov [139], R.J.M. Snellings [59], E.H. Solheim [20], J. Song [17], C. Sonnabend [33,97], F. Soramel [28], A.B. Soto-hernandez [88], R. Spijkers [84], I. Sputowska [107], J. Staa [75], J. Stachel [94], I. Stan [63], P.J. Steffanic [121], S.F. Stiefelmaier [94], D. Stocco [103], I. Storehaug [20], P. Stratmann [137], S. Strazzi [26], A. Sturniolo [31,53], C.P. Stylianidis[84], A.A.P. Suaide [110], C. Suire [130], M. Sukhanov [142], M. Suljic [33], R. Sultanov [142], V. Sumberia [91], S. Sumowidagdo [82], S. Swain[61], I. Szarka [13], M. Szymkowski [135], S.F. Taghavi [95], G. Taillepied [97], J. Takahashi [111], G.J. Tambave [80], S. Tang [6], Z. Tang [119], J.D. Tapia Takaki [117], N. Tapus[125], L.A. Tarasovicova [137], M.G. Tarzila [46], G.F. Tassielli [32], A. Tauro [33], G. Tejeda Muñoz [45], A. Telesca [33], L. Terlizzi [25], C. Terrevoli [115], S. Thakur [4], D. Thomas [108], A. Tikhonov [142], N. Tiltmann [33,137], A.R. Timmins [115], M. Tkacik[106], T. Tkacik [106], A. Toia [64], R. Tokumoto[92], K. Tomohiro[92], N. Topilskaya [142], M. Toppi [49], T. Tork [130], P.V. Torres[65], V.V. Torres [103], A.G. Torres Ramos [32], A. Trifiró [31,53], A.S. Triolo [33,31,53], S. Tripathy [51], T. Tripathy [47], S. Trogolo [33], V. Trubnikov [3], W.H. Trzaska [116], T.P. Trzcinski [135], A. Tumkin [142], R. Turrisi [54], T.S. Tveter [20], K. Ullaland [21], B. Ulukutlu [95], A. Uras [127], G.L. Usai [23], M. Vala[38], N. Valle [22], L.V.R. van Doremalen[59], M. van Leeuwen [84], C.A. van Veen [94], R.J.G. van Weelden [84], P. Vande Vyvre [33], D. Varga [138], Z. Varga [138], M. Vasileiou [78], A. Vasiliev [142], O. Vázquez Doce [49], O. Vazquez Rueda [115], V. Vechernin [142], E. Vercellin [25], S. Vergara Limón[45], R. Verma[47], L. Vermunt [97], R. Vértesi [138], M. Verweij [59], L. Vickovic[34], Z. Vilakazi[122], O. Villalobos Baillie [100], A. Villani [24], A. Vinogradov [142], T. Virgili [29], M.M.O. Virta [116], V. Vislavicius[75], A. Vodopyanov [143], B. Volkel [33], M.A. Völkl [94], K. Voloshin[142], S.A. Voloshin [136], G. Volpe [32], B. von Haller [33], I. Vorobyev [95], N. Vozniuk [142], J. Vrláková [38], J. Wan[40], C. Wang [40], D. Wang[40], Y. Wang [40], Y. Wang [6], A. Wegrzynek [33], F.T. Weiglhofer[39], S.C. Wenzel [33], J.P. Wessels [137], S.L. Weyhmiller [139], J. Wiechula [64], J. Wikne [20], G. Wilk [79], J. Wilkinson [97], G.A. Willems [137], B. Windelband [94], M. Winn [129], J.R. Wright [108], W. Wu[40], Y. Wu [119], R. Xu [6], A. Yadav [43], A.K. Yadav [134],

S. Yalcin [72], Y. Yamaguchi [92], S. Yang[21], S. Yano [92], Z. Yin [6], I.-K. Yoo [17], J.H. Yoon [58], H. Yu[12], S. Yuan[21], A. Yuncu [94], V. Zaccolo [24], C. Zampolli [33], F. Zanone [94], N. Zardoshti [33], A. Zarochentsev [142], P. Závada [62], N. Zaviyalov[142], M. Zhalov [142], B. Zhang [6], C. Zhang [129], L. Zhang [40], S. Zhang [40], X. Zhang [6], Y. Zhang[119], Z. Zhang [6], M. Zhao [10], V. Zherebchevskii [142], Y. Zhi[10], D. Zhou [6], Y. Zhou [83], J. Zhu [97,6], Y. Zhu[6], S.C. Zugravel [56], N. Zurlo [133,55]

Affiliation Notes

[I] Also at: Max-Planck-Institut für Physik, Munich, Germany
[II] Also at: Italian National Agency for New Technologies, Energy and Sustainable Economic Development (ENEA), Bologna, Italy
[III] Also at: Dipartimento DET del Politecnico di Torino, Turin, Italy
[IV] Also at: Department of Applied Physics, Aligarh Muslim University, Aligarh, India
[V] Also at: Institute of Theoretical Physics, University of Wroclaw, Poland
[VI] Also at: An institution covered by a cooperation agreement with CERN

Collaboration Institutes

[1] A.I. Alikhanyan National Science Laboratory (Yerevan Physics Institute) Foundation, Yerevan, Armenia
[2] AGH University of Krakow, Cracow, Poland
[3] Bogolyubov Institute for Theoretical Physics, National Academy of Sciences of Ukraine, Kiev, Ukraine
[4] Bose Institute, Department of Physics and Centre for Astroparticle Physics and Space Science (CAPSS), Kolkata, India
[5] California Polytechnic State University, San Luis Obispo, California, United States
[6] Central China Normal University, Wuhan, China
[7] Centro de Aplicaciones Tecnológicas y Desarrollo Nuclear (CEADEN), Havana, Cuba
[8] Centro de Investigación y de Estudios Avanzados (CINVESTAV), Mexico City and Mérida, Mexico
[9] Chicago State University, Chicago, Illinois, United States
[10] China Institute of Atomic Energy, Beijing, China
[11] China University of Geosciences, Wuhan, China
[12] Chungbuk National University, Cheongju, Republic of Korea
[13] Comenius University Bratislava, Faculty of Mathematics, Physics and Informatics, Bratislava, Slovak Republic
[14] COMSATS University Islamabad, Islamabad, Pakistan
[15] Creighton University, Omaha, Nebraska, United States
[16] Department of Physics, Aligarh Muslim University, Aligarh, India
[17] Department of Physics, Pusan National University, Pusan, Republic of Korea
[18] Department of Physics, Sejong University, Seoul, Republic of Korea
[19] Department of Physics, University of California, Berkeley, California, United States
[20] Department of Physics, University of Oslo, Oslo, Norway
[21] Department of Physics and Technology, University of Bergen, Bergen, Norway
[22] Dipartimento di Fisica, Università di Pavia, Pavia, Italy
[23] Dipartimento di Fisica dell'Università and Sezione INFN, Cagliari, Italy
[24] Dipartimento di Fisica dell'Università and Sezione INFN, Trieste, Italy
[25] Dipartimento di Fisica dell'Università and Sezione INFN, Turin, Italy
[26] Dipartimento di Fisica e Astronomia dell'Università and Sezione INFN, Bologna, Italy
[27] Dipartimento di Fisica e Astronomia dell'Università and Sezione INFN, Catania, Italy
[28] Dipartimento di Fisica e Astronomia dell'Università and Sezione INFN, Padova, Italy
[29] Dipartimento di Fisica 'E.R. Caianiello' dell'Università and Gruppo Collegato INFN, Salerno, Italy
[30] Dipartimento DISAT del Politecnico and Sezione INFN, Turin, Italy
[31] Dipartimento di Scienze MIFT, Università di Messina, Messina, Italy
[32] Dipartimento Interateneo di Fisica 'M. Merlin' and Sezione INFN, Bari, Italy
[33] European Organization for Nuclear Research (CERN), Geneva, Switzerland
[34] Faculty of Electrical Engineering, Mechanical Engineering and Naval Architecture, University of Split, Split, Croatia
[35] Faculty of Engineering and Science, Western Norway University of Applied Sciences, Bergen, Norway

[36] Faculty of Nuclear Sciences and Physical Engineering, Czech Technical University in Prague, Prague, Czech Republic
[37] Faculty of Physics, Sofia University, Sofia, Bulgaria
[38] Faculty of Science, P.J. Šafárik University, Košice, Slovak Republic
[39] Frankfurt Institute for Advanced Studies, Johann Wolfgang Goethe-Universität Frankfurt, Frankfurt, Germany
[40] Fudan University, Shanghai, China
[41] Gangneung-Wonju National University, Gangneung, Republic of Korea
[42] Gauhati University, Department of Physics, Guwahati, India
[43] Helmholtz-Institut für Strahlen- und Kernphysik, Rheinische Friedrich-Wilhelms-Universität Bonn, Bonn, Germany
[44] Helsinki Institute of Physics (HIP), Helsinki, Finland
[45] High Energy Physics Group, Universidad Autónoma de Puebla, Puebla, Mexico
[46] Horia Hulubei National Institute of Physics and Nuclear Engineering, Bucharest, Romania
[47] Indian Institute of Technology Bombay (IIT), Mumbai, India
[48] Indian Institute of Technology Indore, Indore, India
[49] INFN, Laboratori Nazionali di Frascati, Frascati, Italy
[50] INFN, Sezione di Bari, Bari, Italy
[51] INFN, Sezione di Bologna, Bologna, Italy
[52] INFN, Sezione di Cagliari, Cagliari, Italy
[53] INFN, Sezione di Catania, Catania, Italy
[54] INFN, Sezione di Padova, Padova, Italy
[55] INFN, Sezione di Pavia, Pavia, Italy
[56] INFN, Sezione di Torino, Turin, Italy
[57] INFN, Sezione di Trieste, Trieste, Italy
[58] Inha University, Incheon, Republic of Korea
[59] Institute for Gravitational and Subatomic Physics (GRASP), Utrecht University/Nikhef, Utrecht, Netherlands
[60] Institute of Experimental Physics, Slovak Academy of Sciences, Košice, Slovak Republic
[61] Institute of Physics, Homi Bhabha National Institute, Bhubaneswar, India
[62] Institute of Physics of the Czech Academy of Sciences, Prague, Czech Republic
[63] Institute of Space Science (ISS), Bucharest, Romania
[64] Institut für Kernphysik, Johann Wolfgang Goethe-Universität Frankfurt, Frankfurt, Germany
[65] Instituto de Ciencias Nucleares, Universidad Nacional Autónoma de México, Mexico City, Mexico
[66] Instituto de Física, Universidade Federal do Rio Grande do Sul (UFRGS), Porto Alegre, Brazil
[67] Instituto de Física, Universidad Nacional Autónoma de México, Mexico City, Mexico
[68] iThemba LABS, National Research Foundation, Somerset West, South Africa
[69] Jeonbuk National University, Jeonju, Republic of Korea
[70] Johann-Wolfgang-Goethe Universität Frankfurt Institut für Informatik, Fachbereich Informatik und Mathematik, Frankfurt, Germany
[71] Korea Institute of Science and Technology Information, Daejeon, Republic of Korea
[72] KTO Karatay University, Konya, Turkey
[73] Laboratoire de Physique Subatomique et de Cosmologie, Université Grenoble-Alpes, CNRS-IN2P3, Grenoble, France
[74] Lawrence Berkeley National Laboratory, Berkeley, California, United States
[75] Lund University Department of Physics, Division of Particle Physics, Lund, Sweden
[76] Nagasaki Institute of Applied Science, Nagasaki, Japan
[77] Nara Women's University (NWU), Nara, Japan
[78] National and Kapodistrian University of Athens, School of Science, Department of Physics , Athens, Greece
[79] National Centre for Nuclear Research, Warsaw, Poland
[80] National Institute of Science Education and Research, Homi Bhabha National Institute, Jatni, India
[81] National Nuclear Research Center, Baku, Azerbaijan
[82] National Research and Innovation Agency - BRIN, Jakarta, Indonesia
[83] Niels Bohr Institute, University of Copenhagen, Copenhagen, Denmark
[84] Nikhef, National institute for subatomic physics, Amsterdam, Netherlands
[85] Nuclear Physics Group, STFC Daresbury Laboratory, Daresbury, United Kingdom
[86] Nuclear Physics Institute of the Czech Academy of Sciences, Husinec-Řež, Czech Republic
[87] Oak Ridge National Laboratory, Oak Ridge, Tennessee, United States

[88] Ohio State University, Columbus, Ohio, United States

[89] Physics department, Faculty of science, University of Zagreb, Zagreb, Croatia

[90] Physics Department, Panjab University, Chandigarh, India

[91] Physics Department, University of Jammu, Jammu, India

[92] Physics Program and International Institute for Sustainability with Knotted Chiral Meta Matter (SKCM2), Hiroshima University, Hiroshima, Japan

[93] Physikalisches Institut, Eberhard-Karls-Universität Tübingen, Tübingen, Germany

[94] Physikalisches Institut, Ruprecht-Karls-Universität Heidelberg, Heidelberg, Germany

[95] Physik Department, Technische Universität München, Munich, Germany

[96] Politecnico di Bari and Sezione INFN, Bari, Italy

[97] Research Division and ExtreMe Matter Institute EMMI, GSI Helmholtzzentrum für Schwerionenforschung GmbH, Darmstadt, Germany

[98] Saga University, Saga, Japan

[99] Saha Institute of Nuclear Physics, Homi Bhabha National Institute, Kolkata, India

[100] School of Physics and Astronomy, University of Birmingham, Birmingham, United Kingdom

[101] Sección Física, Departamento de Ciencias, Pontificia Universidad Católica del Perú, Lima, Peru

[102] Stefan Meyer Institut für Subatomare Physik (SMI), Vienna, Austria

[103] SUBATECH, IMT Atlantique, Nantes Université, CNRS-IN2P3, Nantes, France

[104] Sungkyunkwan University, Suwon City, Republic of Korea

[105] Suranaree University of Technology, Nakhon Ratchasima, Thailand

[106] Technical University of Košice, Košice, Slovak Republic

[107] The Henryk Niewodniczanski Institute of Nuclear Physics, Polish Academy of Sciences, Cracow, Poland

[108] The University of Texas at Austin, Austin, Texas, United States

[109] Universidad Autónoma de Sinaloa, Culiacán, Mexico

[110] Universidade de São Paulo (USP), São Paulo, Brazil

[111] Universidade Estadual de Campinas (UNICAMP), Campinas, Brazil

[112] Universidade Federal do ABC, Santo Andre, Brazil

[113] University of Cape Town, Cape Town, South Africa

[114] University of Derby, Derby, United Kingdom

[115] University of Houston, Houston, Texas, United States

[116] University of Jyväskylä, Jyväskylä, Finland

[117] University of Kansas, Lawrence, Kansas, United States

[118] University of Liverpool, Liverpool, United Kingdom

[119] University of Science and Technology of China, Hefei, China

[120] University of South-Eastern Norway, Kongsberg, Norway

[121] University of Tennessee, Knoxville, Tennessee, United States

[122] University of the Witwatersrand, Johannesburg, South Africa

[123] University of Tokyo, Tokyo, Japan

[124] University of Tsukuba, Tsukuba, Japan

[125] University Politehnica of Bucharest, Bucharest, Romania

[126] Université Clermont Auvergne, CNRS/IN2P3, LPC, Clermont-Ferrand, France

[127] Université de Lyon, CNRS/IN2P3, Institut de Physique des 2 Infinis de Lyon, Lyon, France

[128] Université de Strasbourg, CNRS, IPHC UMR 7178, F-67000 Strasbourg, France, Strasbourg, France

[129] Université Paris-Saclay, Centre d'Etudes de Saclay (CEA), IRFU, Départment de Physique Nucléaire (DPhN), Saclay, France

[130] Université Paris-Saclay, CNRS/IN2P3, IJCLab, Orsay, France

[131] Università degli Studi di Foggia, Foggia, Italy

[132] Università del Piemonte Orientale, Vercelli, Italy

[133] Università di Brescia, Brescia, Italy

[134] Variable Energy Cyclotron Centre, Homi Bhabha National Institute, Kolkata, India

[135] Warsaw University of Technology, Warsaw, Poland

[136] Wayne State University, Detroit, Michigan, United States

[137] Westfälische Wilhelms-Universität Münster, Institut für Kernphysik, Münster, Germany

[138] Wigner Research Centre for Physics, Budapest, Hungary

[139] Yale University, New Haven, Connecticut, United States

[140] Yonsei University, Seoul, Republic of Korea

[141] Zentrum für Technologie und Transfer (ZTT), Worms, Germany

[142] Affiliated with an institute covered by a cooperation agreement with CERN

[143] Affiliated with an international laboratory covered by a cooperation agreement with CERN.